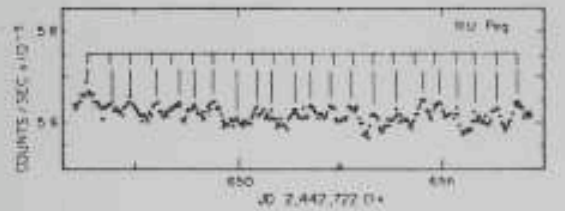

FIG. 1.—Portion of the light curve of RU Peg from run 1677. The individual maxima of the 50 s quasi-periodic oscillation are marked to illustrate its lack of short-term coherence. The inset scale corresponds to a period of 51.7 s, the mean period during the illustrated portion of the light curve.

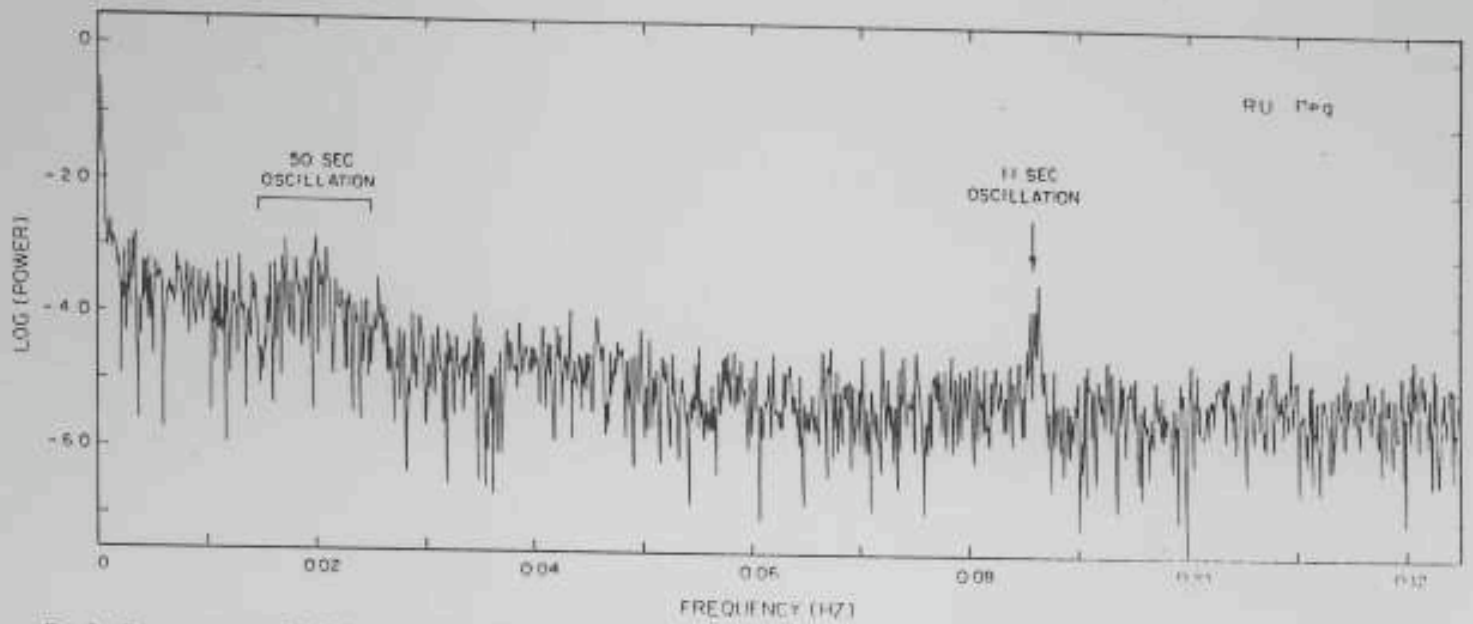

FIG. 2.—Power spectrum of the light curve of RU Peg from run 1677, showing the short-period coherent oscillation at 0.09 Hz and the quasi-periodic oscillation at 0.02 Hz.

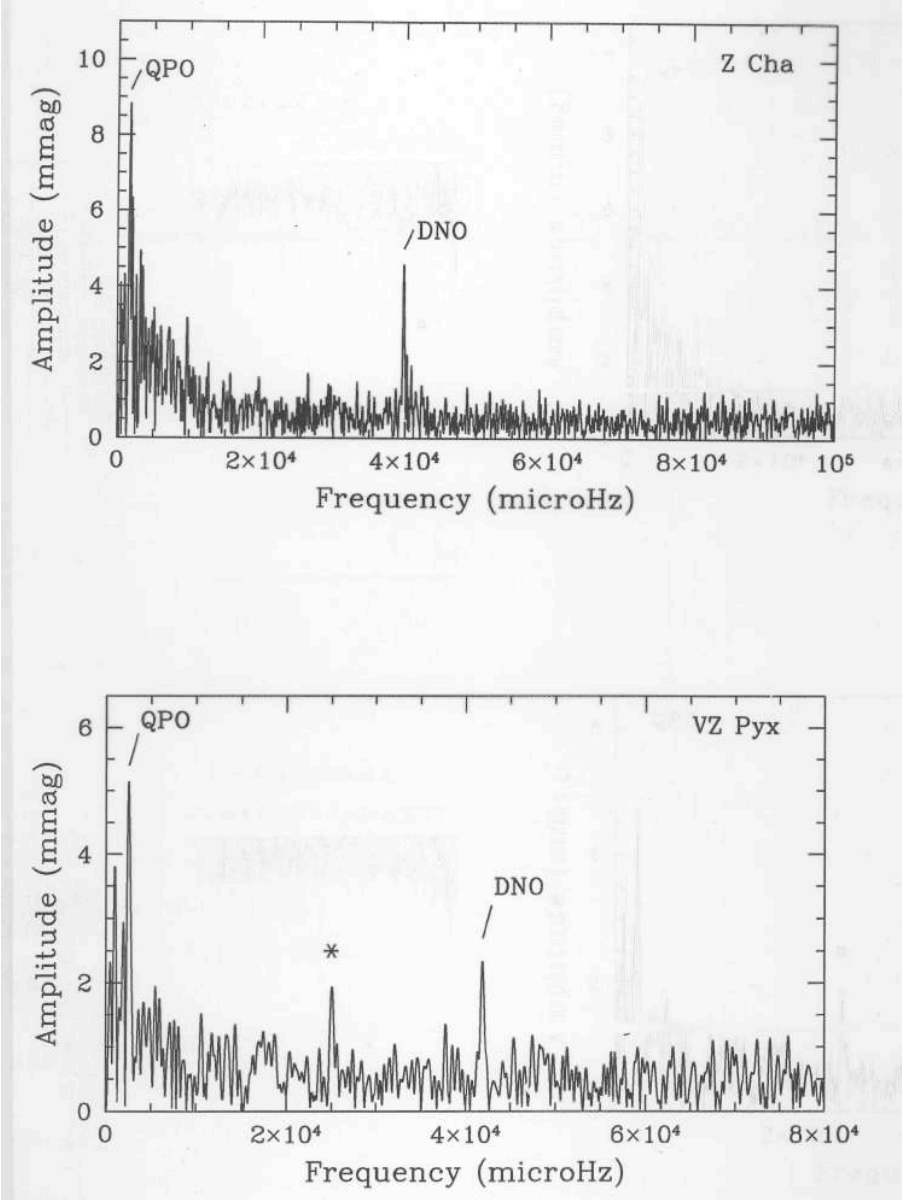
Z Cha
QPO
DNO
Amplitude (mmag)
Frequency (microHz)
0
2
4
6
8
10
2×10⁴
4×10⁴
6×10⁴
8×10⁴
10⁵
VZ Pyx
QPO
DNO
*
Amplitude (mmag)
Frequency (microHz)
0
2
4
6
2×10⁴
4×10⁴
6×10⁴
8×10⁴

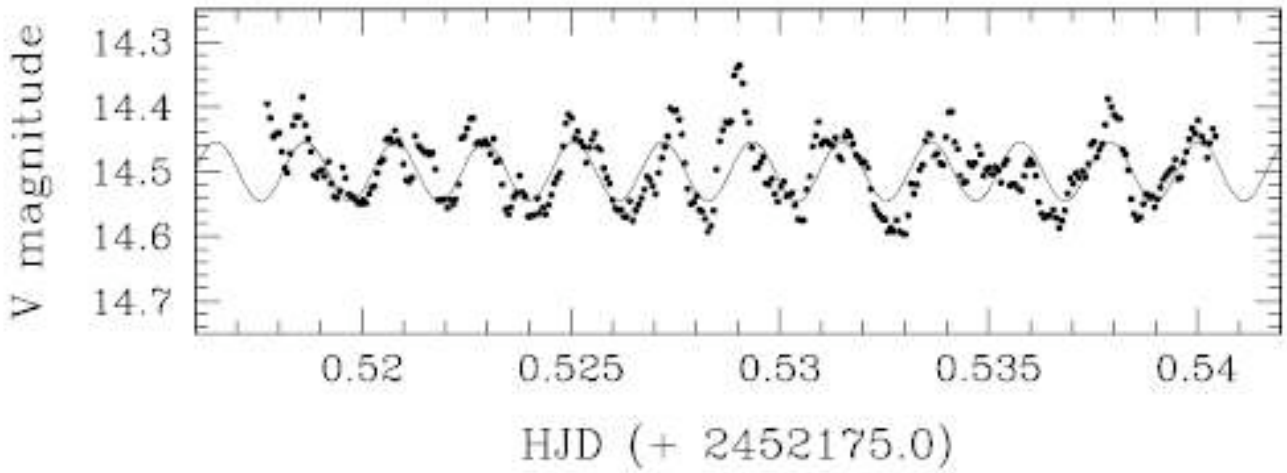

FIGURE 4. The light curve of WX Hyi showing the 185-s QPO clearly Superimposed is the result from the non-linear sinusoidal least-squares fit (reproduced from [6]).

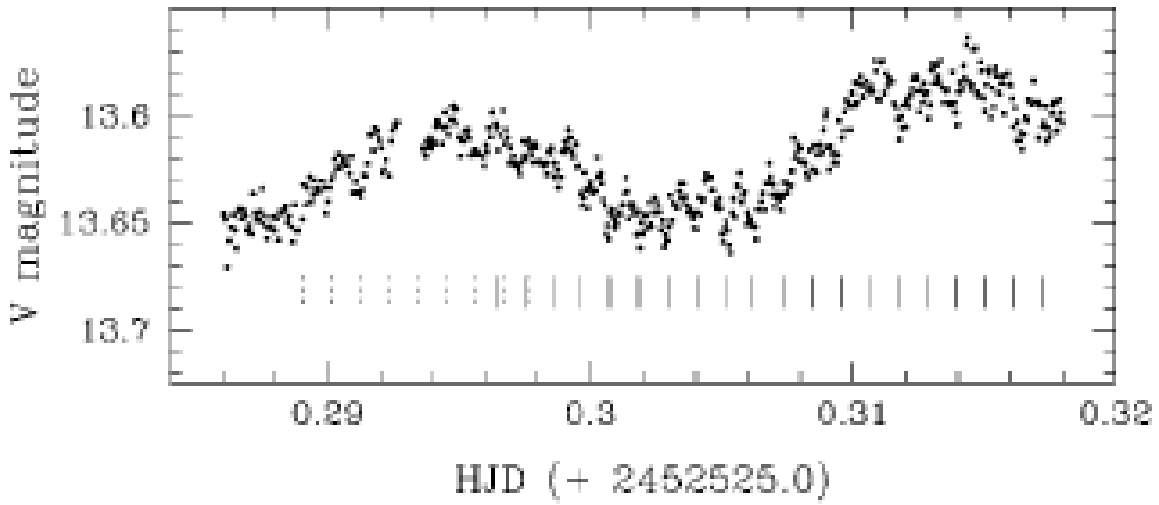

FIG. 4.—Light curve of EC 2117-54 (the first 45 minutes of run S6554). The lpDNO modulation at 94.21 s is clearly visible in the light curve. The lpDNO minima are marked by vertical bars. There is a phase shift around HJD 2,452,525.297. (From WWP03.)

RAPID OPTICAL AND ULTRAVIOLET MODULATIONS IN CATACLYSMIC VARIABLES

Star	Type	P_{orb} (h)	DNO (s)	lpDNO (s)	QPO (s)	References
SS Cyg	DN	6.60	6.58* – 10.9	32-36	83-111,730	1,2,15,16,53
RU Peg	DN	8.99	11.6 – 11.8 → ?		~51	
VW Hyi	NL	1.78	14.03 – 40	~90	400-600	3,4,5
EM Cyg	DN	6.98	14.6 – 21.2			
Z Cam	DN	6.96	16.0 – 18.8			
HX Peg	DN	4.82	16.2-16.4	~83	1400-1900	5
WX Cet	DN	1.40	17.4			60
OY Car	DN	1.50	17.6 – 28.0		~320	5,6
WX Hyi	DN	1.80	19.4		~190,1140,1560	5
V436 Cen	DN	1.50	19.5 – 20.1		475	4,5
HL Aqr	NL	3.25	19.6			
HT Cas	DN	1.77	20.2 – 20.4	~100		1
RR Pic	N	3.48	20 – 40			
TU Men	DN	2.82	20.6		313	7
HP Lib	AMC	0.31			~ 290	59
CR Boo	AMC	0.40	21 - 23	62	~300	5
AQ Eri	DN	1.46	21.0 – 23.5	~90	~280	5
AH Hya	DN	-	21.55			7
BR Lup	DN	1.91	21.65			7
SW UMa	DN	1.36	22.3		280-370	41
KT Per	DN	3.92	22.4 – 29.3	~86,147		
EC2117	NL	3.71	22.5 – 25.5	~95	~500	5
SY Cnc	DN	9.12	23.3 – 33.0			
VZ Pyx	DN	1.78	23.9	112	390, ~3000	5,29
V803 Cen	AMC	0.28		176		5
V1159 Ori	DN	1.50	24 – 34	177	→?	7,42
AH Her	DN	5.93	24.0 – 38.8	~100		1
CN Ori	DN	3.91	24.3 – 32.6			5
IX Vel	N	4.65	24.6 – 29.1		~500	25
U Gem	DN	4.25	~25	~146		26
Z Cha	DN	1.79	25.1 -27.7		585	5
V893 Sco	DN	1.82	25.2		~350	5,30
TY PsA	DN	2.02	25.5 - 30			
BP Lyn	NL	3.67	25.5			
AM CVn	AMC	0.28	26.3		290,820	55,56,57,58
WZ Sge	DN	1.36	27.87, 28.95		742	4,8,9,10,11,12,13,
			14.48 + others			14,31,45,46,47
V2051 Oph	DN	1.50	28.06, 29.77		486,1800	4,18
			42.2			

Star	Type	P_{orb} (h)	Period (s)	Energy	State	References
SS Cyg	DN	6.60	7.4–10.7	soft	O	1–4
			2.8*	soft	O	5
			155–245	hard	O	6
VW Hyi	DN	1.78	14.06, 14.2–14.4	soft	O	7
			63–68	soft	O	7
			~60	hard	Q	8
			~500	hard	O	9
HT Cas	DN	1.77	21.85:	hard	Q	10, 11
U Gem	DN	4.25	25–29	soft	O	2, 12
			121, 135	hard	Q	11
			585	hard	O	11
WZ Sge	DN	1.36	27.8	hard	Q	13
SU UMa	DN	1.83	33.93:	hard	Q	10
YZ Cnc	DN	2.21	222	hard	Q	11
RW Sex	NL	5.93	254	hard		11
AB Dra	DN	3.65	290	hard	O	11
OY Car	DN	1.50	2240	soft	Q	14
GK Per	N, DN	1.99d	3000–5000	hard	O	15, 16

NOTES—O = outburst, Q = quiescence. A colon denotes a less-certain observation; asterisk denotes cases in which frequency doubling had occurred.

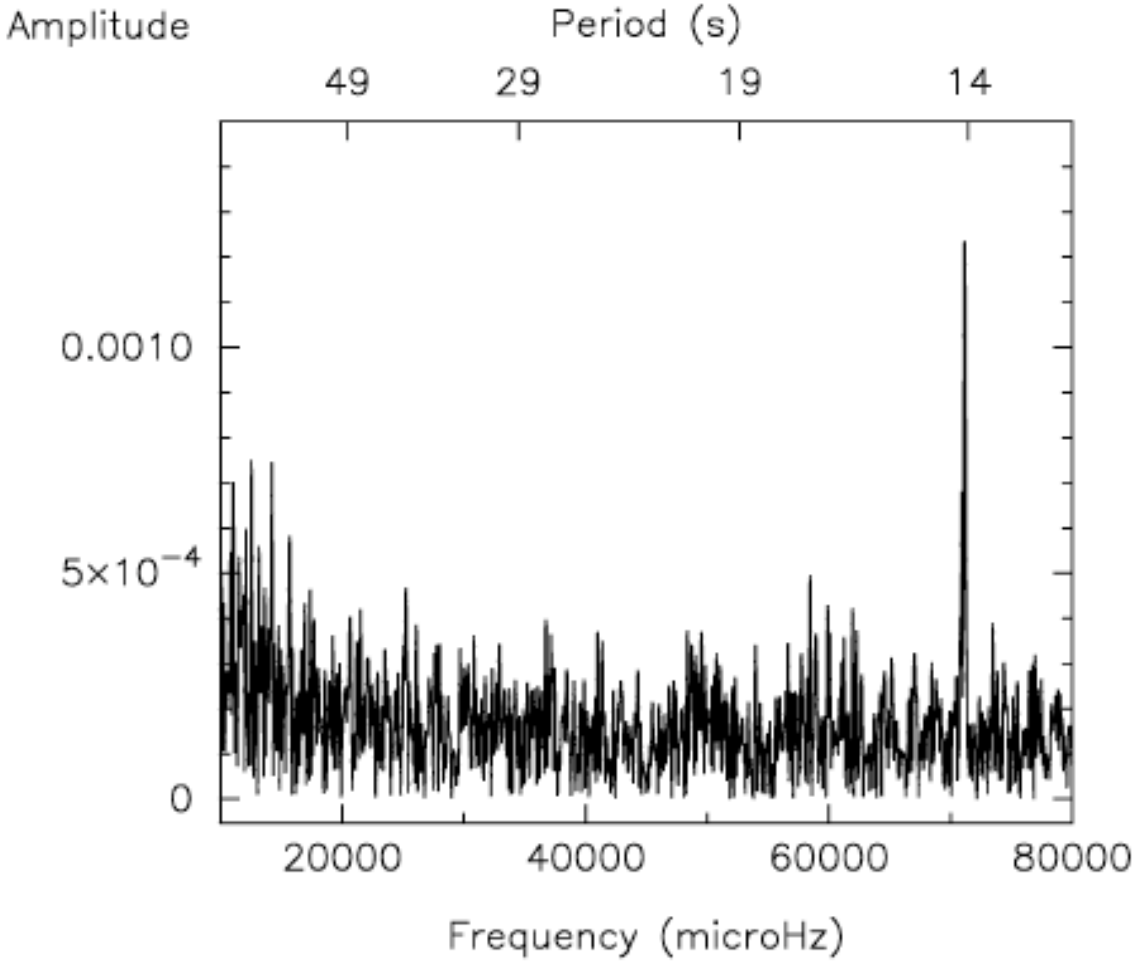

Figure 6. Fourier amplitude spectrum of the light curve of VW Hyi on 1982 December 19.

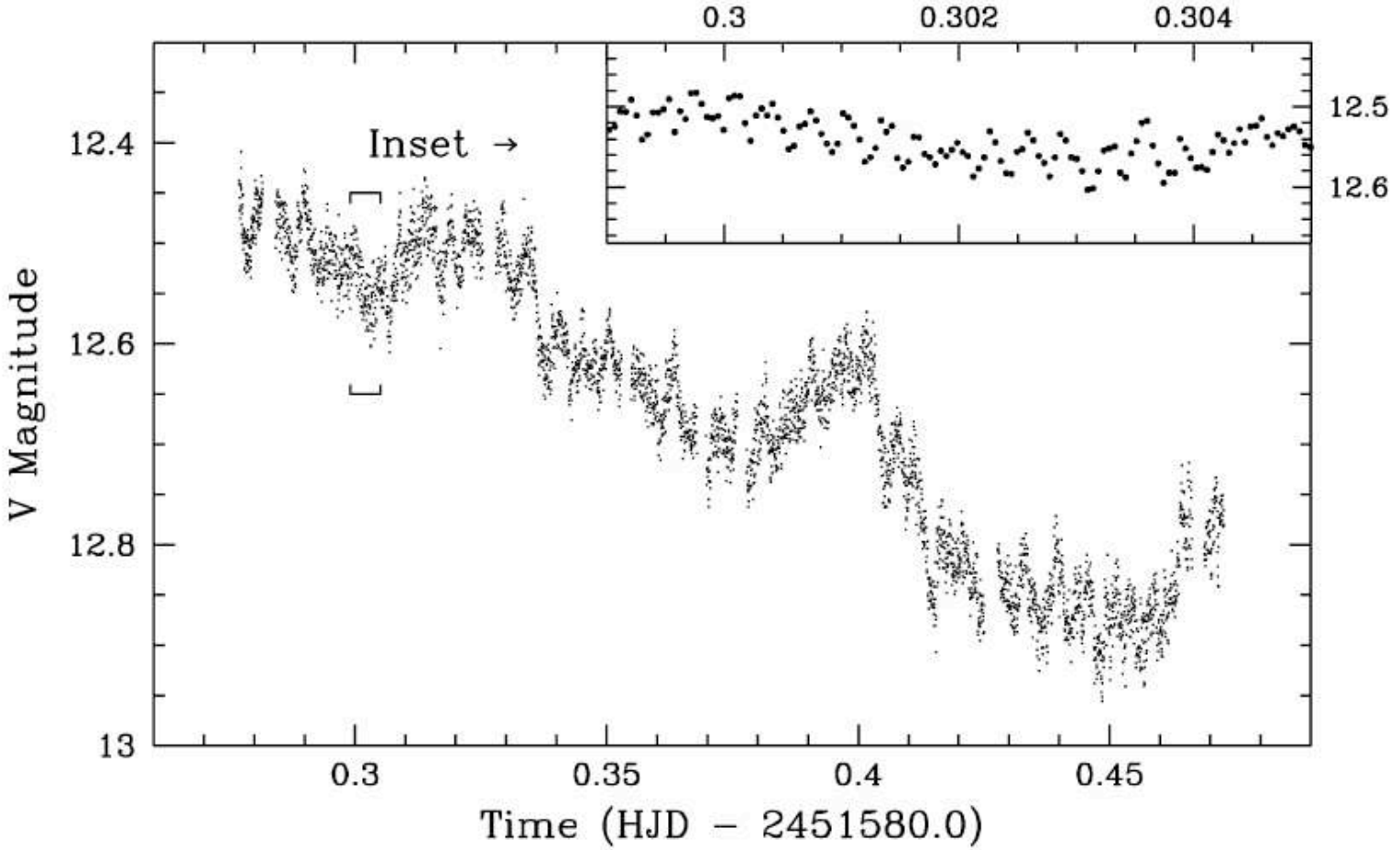

Figure 1. The light curve of VW Hyi on 2000 February 5, taken during the late-decay phase of this dwarf nova outburst. The inset is an amplified view of a small part, showing the DNOs.

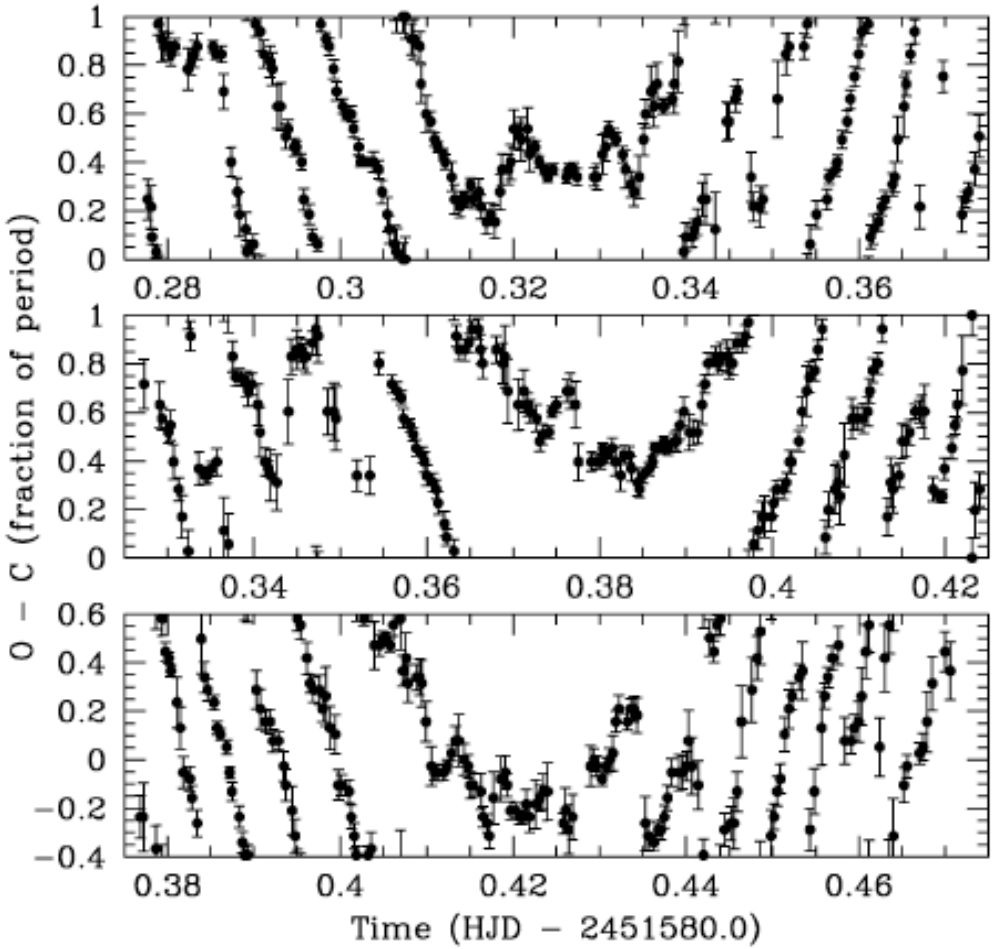

Figure 10. Three O−C diagrams for the DNOs present in Fig. 1. The 'oak panel' effect is obtained by analysing separately the first half of the run (top), the central half (middle) and the final half (bottom).

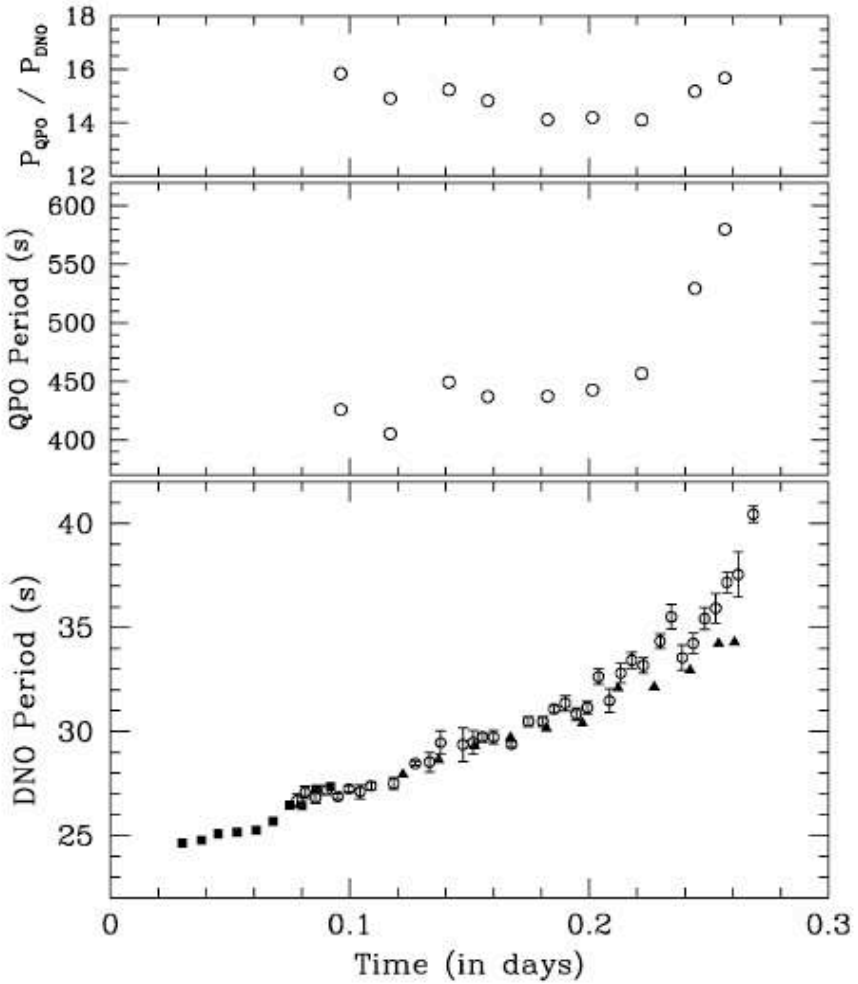

Figure 3. Variations with time of the DNO and QPO periods in the normal outburst of 2000 February (circles with error bars). DNOs are added for the superoutburst of 1972 December (triangles) and the normal outburst of 2001 February (squares). The topmost panel shows the ratio of the periods in the 2000 February run.

Table 1. An overview of our data archive of VW Hyi. Observations during outburst.

Run	Date	Outburst type	Phase (d)	Length (h)	DNO	QPO	Remarks
S0110	1972 Dec 10	Super	−14.85	2.47	No	No	Early rise to supermaximum, no DNOs $> 1.0\times10^{-3}$
S0111	1972 Dec 10	Super	−14.77	0.97	No	No	Rise to supermaximum, no DNOs $> 9\times10^{-4}$
S0112	1972 Dec 10	Super	−14.67	2.31	No	No	Final rise to supermaximum, no DNOs $> 7\times10^{-4}$
S2230	1975 Dec 9	Super	−13.33	0.68	No	–	No DNOs $> 1.0\times10^{-3}$
S2233	1975 Dec 10	Super	−12.40	0.59	No	–	No DNOs $> 2.5\times10^{-3}$
S3434	1984 Oct 24	Super	−11.70	3.65	No	No	At supermaximum, no DNOs $> 7\times10^{-4}$
S2241	1975 Dec 11	Super	−11.34	2.63	No	Yes?	No DNOs $> 1.8\times10^{-3}$, some evidence for QPO at 745 s towards the end of the run
S3435	1984 Oct 25	Super	−10.70	3.68	No	–	No DNOs $> 1.1\times10^{-3}$
S2243	1975 Dec 12	Super	−10.36	1.65	No	Yes	Probable QPO at 425 s. No DNOs $> 1.1\times10^{-3}$
S3436	1984 Oct 26	Super	−9.79	2.06	Yes	No	DNO at 14.29 s (3.5×10^{-3}) in first 50 min
S0115	1972 Dec 18	Super	−6.86	1.20	No	No	No DNOs $> 6\times10^{-4}$
S3078	1982 Dec 19	Super	−5.32	1.95	Yes	No	Stable DNO at 14.06 s, ampl. 1.2×10^{-3}
S0480	1973 Nov 30	Super	−5.19	1.73	No	No	No DNOs $> 2.5\times10^{-3}$
S0118	1972 Dec 20	Super	−4.86	1.93	No	No	No DNOs $> 9\times10^{-4}$
S3437	1984 Oct 31	Super	−4.62	2.90	No	–	No DNOs $> 1.2\times10^{-3}$
S0120	1972 Dec 21	Super	−3.87	2.03	No	No	No DNOs $> 8\times10^{-4}$
S3692	1985 Nov 8	Super	−3.81	0.36	No	–	No DNOs $> 1.4\times10^{-3}$
S3693	1985 Nov 8	Super	−3.80	0.29	No	–	No DNOs $> 1.3\times10^{-3}$
S3438	1984 Nov 1	Super	−3.75	1.94	No	No	No DNOs $> 1.5\times10^{-3}$
S2911	1981 Nov 25	Normal (L)	−2.71	3.14	No	No	Final rise to normal maximum, no DNOs $> 8\times10^{-4}$
S2621	1978 Jan 3	Normal (M)	−2.26	2.75	No	No	Final rise to normal maximum, no DNOs $> 7\times10^{-4}$
S0122	1972 Dec 23	Super	−1.82	2.56	No	Yes	QPO at 410 s in first half of the run (3×10^{-3}) No DNOs $> 5\times10^{-4}$
S1277	1974 Oct 31	Normal (?)	−1.77	1.78	No	No	At normal maximum, no DNOs $> 1.3\times10^{-4}$
S1571	1974 Dec 20	Super	−1.04	1.99	No	Yes?	Start of fall from supermaximum plateau. Possible QPO at 1151 s (4.2×10^{-3}). No DNOs $> 1.3\times10^{-3}$
S6183	2001 Feb 15	Normal (L)	−0.94	1.68	No	No	No DNOs $> 1.3\times10^{-3}$
S3703	1985 Nov 11	Super	−0.83	1.04	No	No	No DNOs $> 2.6\times10^{-3}$
S0124	1972 Dec 24	Super	−0.79	1.84	No	No	No DNOs $> 8\times10^{-4}$
S2914	1981 Nov 27	Normal (L)	−0.73	0.52	No	No	No DNOs $> 2.2\times10^{-3}$
S3410	1984 Sep 22	Normal (M)	−0.58	0.51	No	–	No DNOs $> 1.7\times10^{-3}$
S1307	1974 Nov 2	Normal (M)	−0.3*	1.33	Yes	Yes	QPOs at ∼185 s (3.5×10^{-3}). DNOs at ∼18.2 s, frequent small period changes. Average 2×10^{-3}, max. 8×10^{-3}
S0018	1972 Sep 11	Normal (L)	−0.11	2.04	Yes	No	DNOs lengthening (20.2–20.6 s, ampl. 2.2×10^{-3})
S1594	1974 Dec 21	Super	−0.05	2.77	No	No	No DNOs $> 1.3\times10^{-3}$
S6184	2001 Feb 16	Normal (L)	0.06	1.68	Yes	Yes	DNO evolution (24.6 → 27.4 s), see discussion in text
S2915	1981 Nov 28	Normal (L)	0.10	0.73	Yes	No	Average DNO at 21.3 s, short coherence (∼660 s). Range in DNO period 20.6–22.4 s
S0127	1972 Dec 25	Super	0.17	3.77	Yes	Yes	DNO evolution (28 → 34 s), see discussion in text
S6059	2000 Feb 5	Normal (M)	0.18	5.27	Yes	Yes	DNO (27 → 40 s) / QPO evolution, see discussion in text
S6138	2000 Dec 19	Normal (M)	0.54	7.63	Yes	Yes	DNOs in range 25–34 s of short coherence (∼1260 s)
S3416	1984 Sep 23	Normal (M)	0.56	1.19	Yes	Yes	DNOs in range 25–30 s of short coherence. Modulation at QPO period of 300 s (see text)
S1322	1974 Nov 3	Normal (M)	0.7*	4.91	Yes	Yes	DNOs in range 26–33 s. See WB
S5248	1990 Nov 6	Normal (M)	0.76	4.66	Yes	Yes	QPO at 2100 s + first and second harmonic, see text Occasional DNOs near 40 s of low coherence
S2623	1978 Jan 6	Normal (M)	0.78	3.60	Yes	Yes	DNOs in range 22–27 s. See RW
S0484	1973 Dec 6	Super	0.79	3.91	Yes	Yes	Strong QPO at 1326 s (4.4×10^{-2}), see Fig. 12 DNOs in range of 29–38 s of short coherence, see text
S0019	1972 Sep 12	Normal (L)	0.94	4.30	Yes	Yes	Large amplitude QPOs at ∼500 s (2.5×10^{-2})
S1616	1974 Dec 22	Super	0.96	2.27	No	No	No DNOs $> 2.5\times10^{-3}$
S0129	1973 Jan 8	Normal (S)	1.04	2.14	No	No	No DNOs $> 4.5\times10^{-3}$
S6060	2000 Feb 6	Normal (M)	1.11	1.53	No	No	No DNOs $> 5\times10^{-3}$
S0026	1972 Sep 13	Normal (L)	1.92	3.32	No	Yes	QPOs at 1043 s (2.4×10^{-2})
S0128	1972 Dec 27	Super	2.14	1.86	No	No	No DNOs $> 4\times10^{-3}$
S3715	1985 Nov 14	Super	2.26	1.27	Yes	Yes	DNOs at 24.7 s (3.4×10^{-3}) and QPOs at ∼360 s in last hour of run
S2917	1981 Nov 30	Normal (L)	2.34	2.18	No	No	No DNOs $> 2.6\times10^{-3}$
S0030	1972 Sep 14	Normal (L)	2.96	6.92	No	Yes	Evidence for QPO behaviour, but of low coherence Several cycles at 1140 s (2.5×10^{-2})
S0077	1972 Oct 11	Quiescence		4.11	No	Yes?	Some evidence for occasional QPO at 935 s No DNOs $> 4\times10^{-3}$
S0085	1972 Oct 13	Quiescence		1.67	No	Yes?	Evidence for few cycles of QPO at 720 s No DNOs $> 6\times10^{-3}$
S0093	1972 Oct 14	Quiescence		3.33	No		No DNOs $> 3.5\times10^{-3}$
S0073	1972 Nov 26	Quiescence		2.83	No	Yes?	Possible QPO at 260 s. No DNOs $> 5\times10^{-3}$
S0102	1972 Dec 5	Quiescence		1.31	No	Yes	QPO at 833 s + first harmonic. No DNOs $> 4.5\times10^{-3}$
S0105	1972 Dec 8	Quiescence		1.80	No	Yes	QPO near 600 s + first harmonic (2.5×10^{-3}) No DNOs $> 2.5\times10^{-3}$
S1414	1974 Dec 2	Quiescence		2.89	No	Yes?	Evidence for QPO of short coherence at 980 s No DNOs $> 2.5\times10^{-3}$

* Our relative magnitudes taken from photoelectric photometry have been used to determine the phase of our observations on these dates with respect to the outburst template. This outburst was sparsely sampled by the observers who reported to the RASNZ.

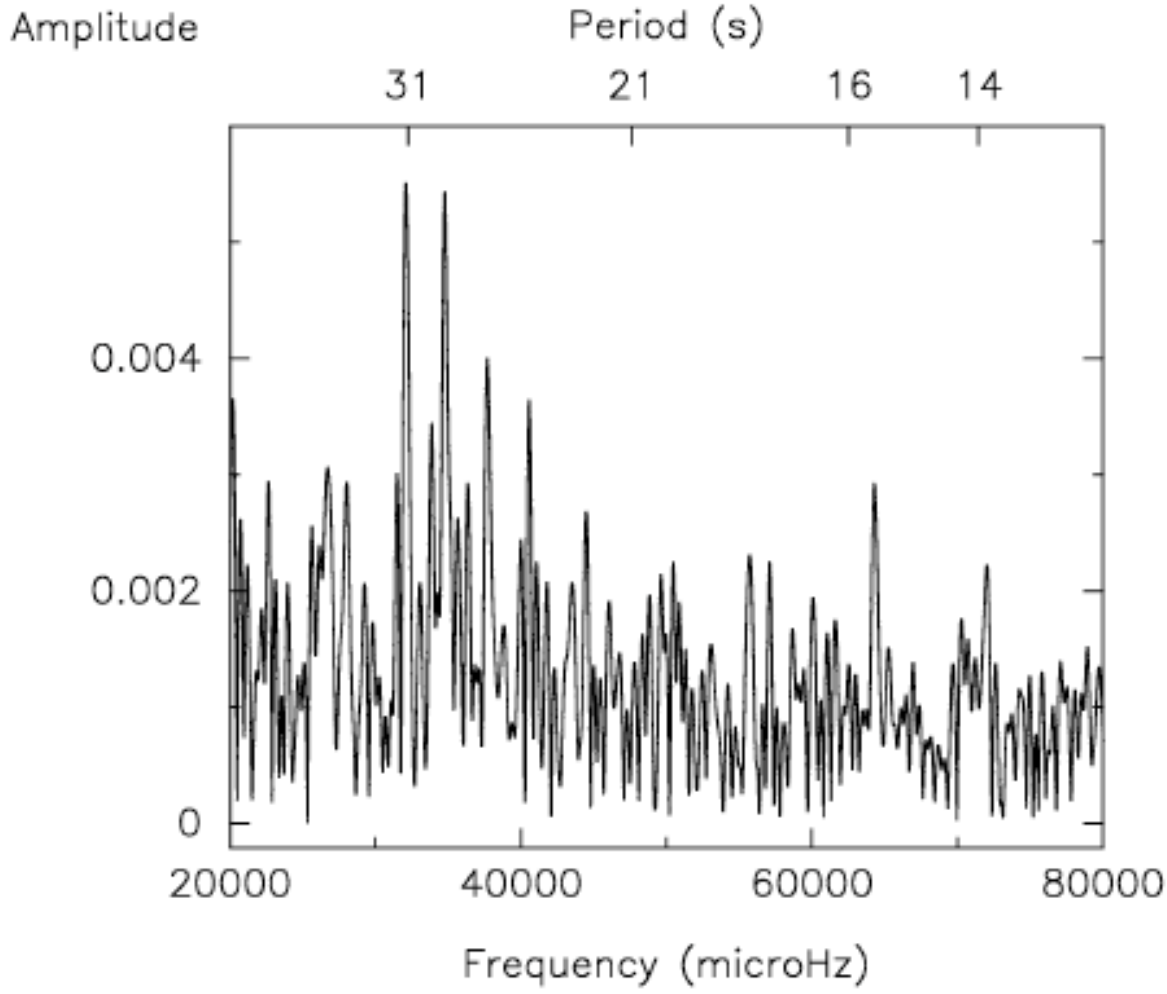

Figure 18. Fourier spectrum of the first 45 min of the light curve on 1974 November 3.

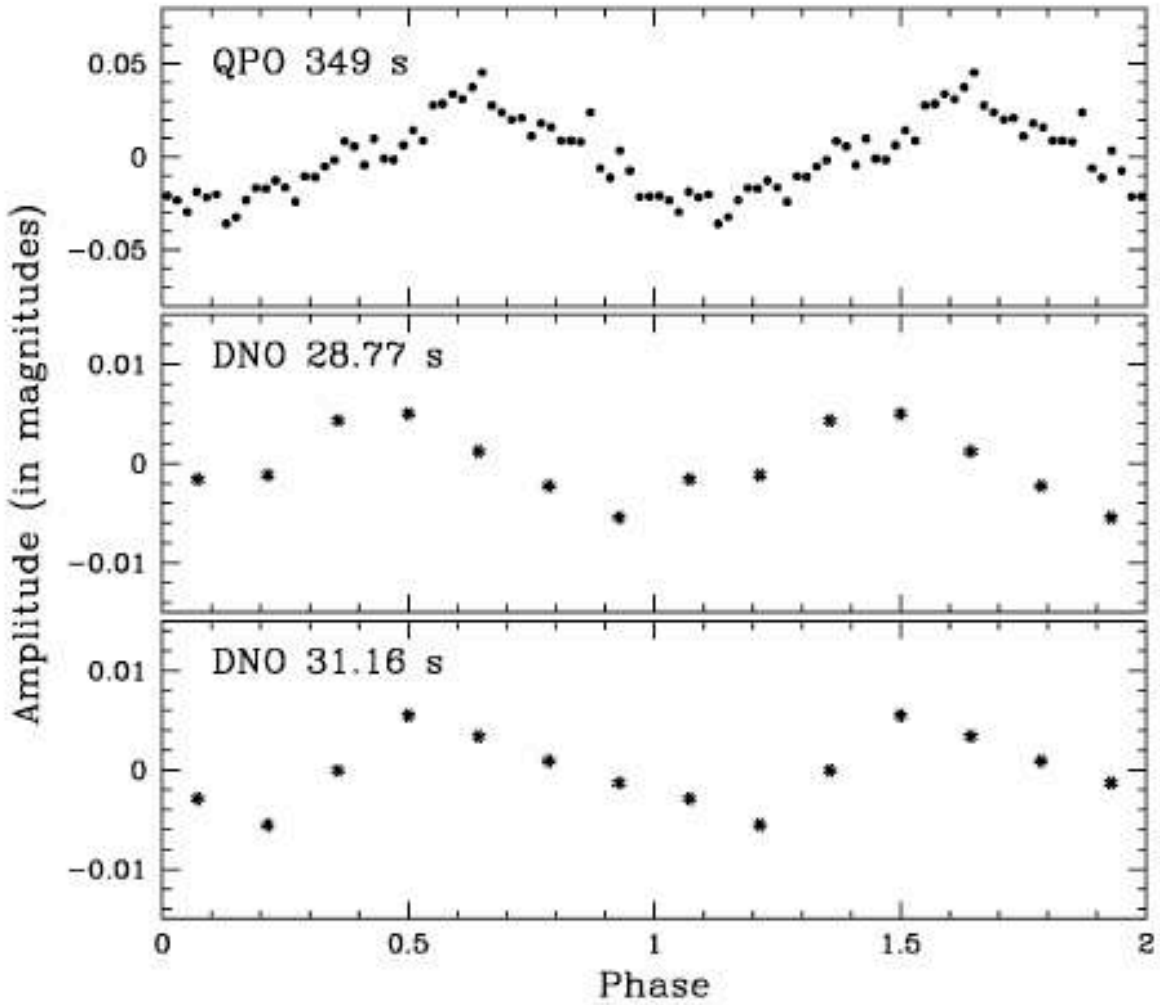

Figure 19. Averaged profiles of the QPOs and DNOs illustrated in Fig. 18.

VW Hyi : EUV Superoutburst

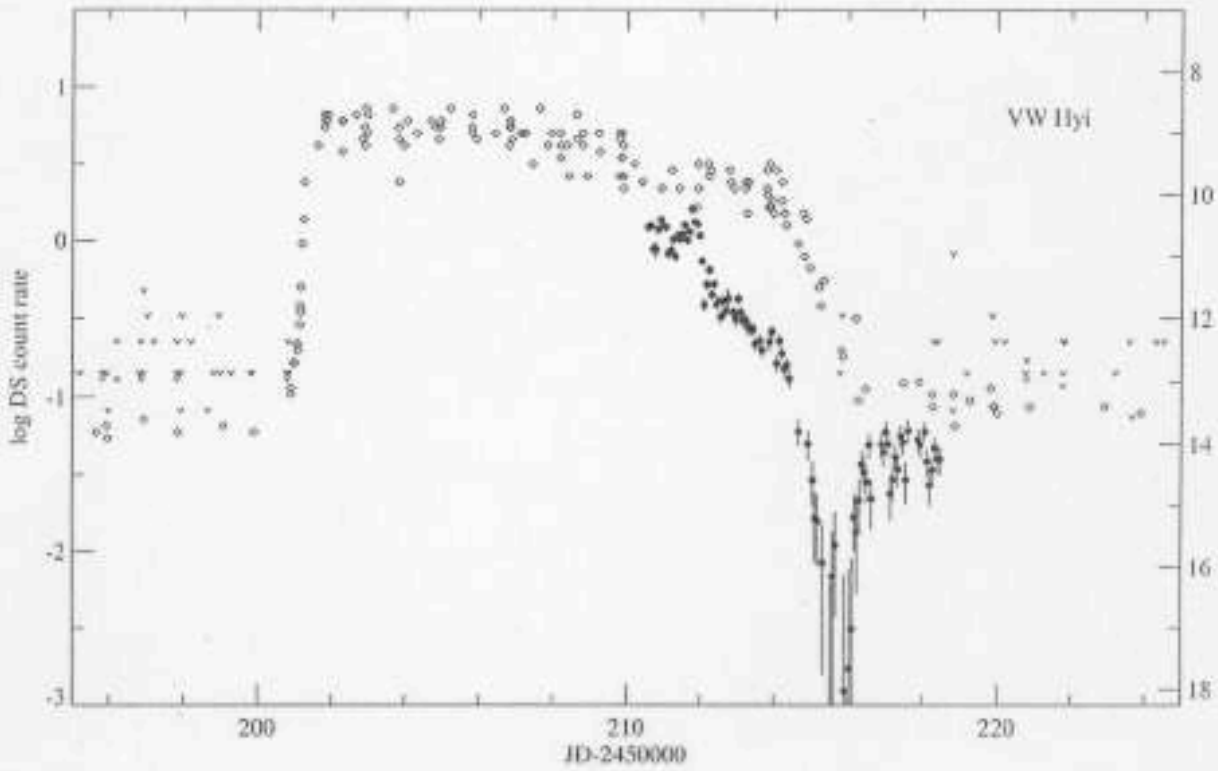

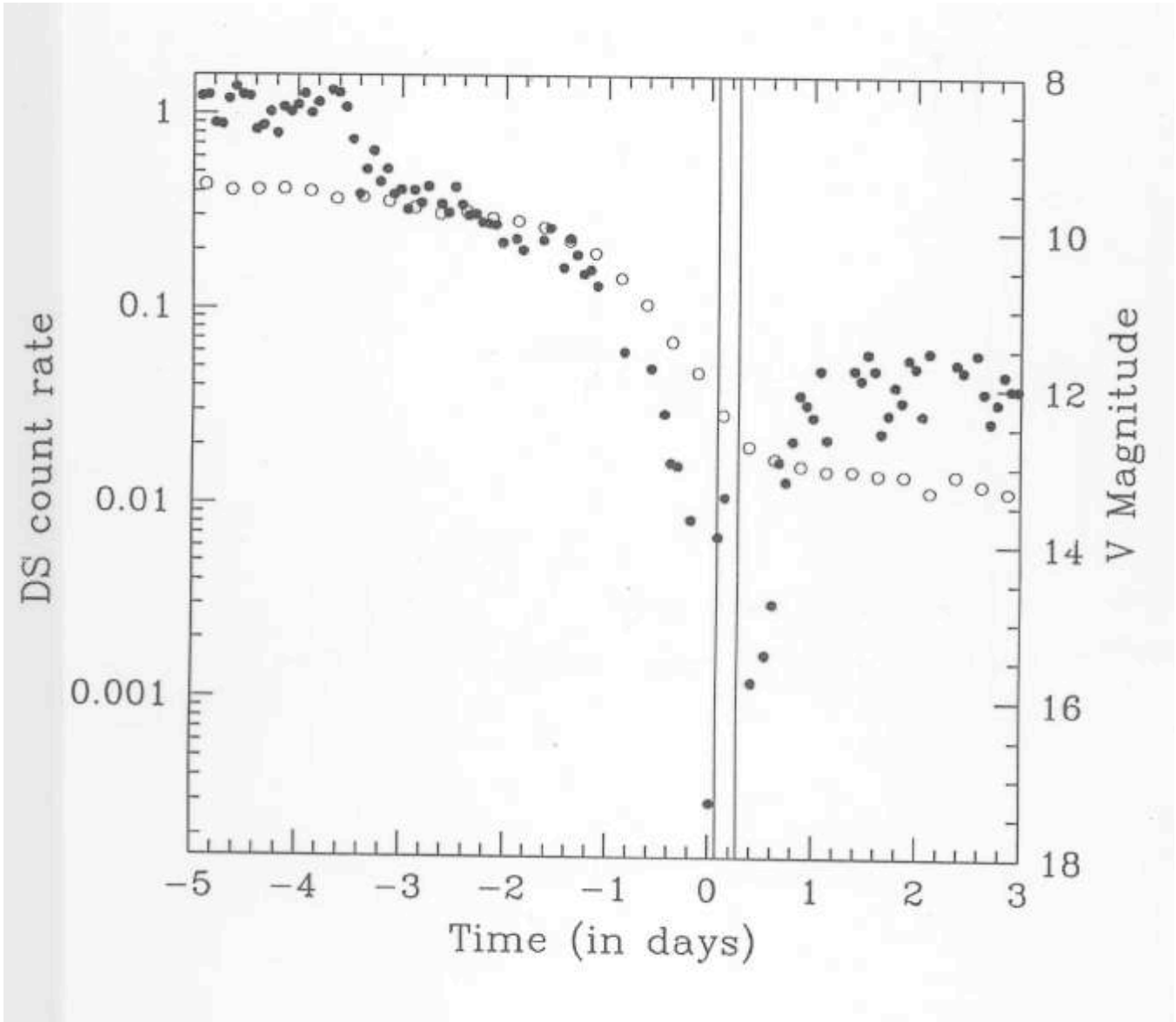
DS count rate
1
0.1
0.01
0.001
8
10
12
14
16
18
V Magnitude
−5
−4
−3
−2
−1
0
1
2
3
Time (in days)

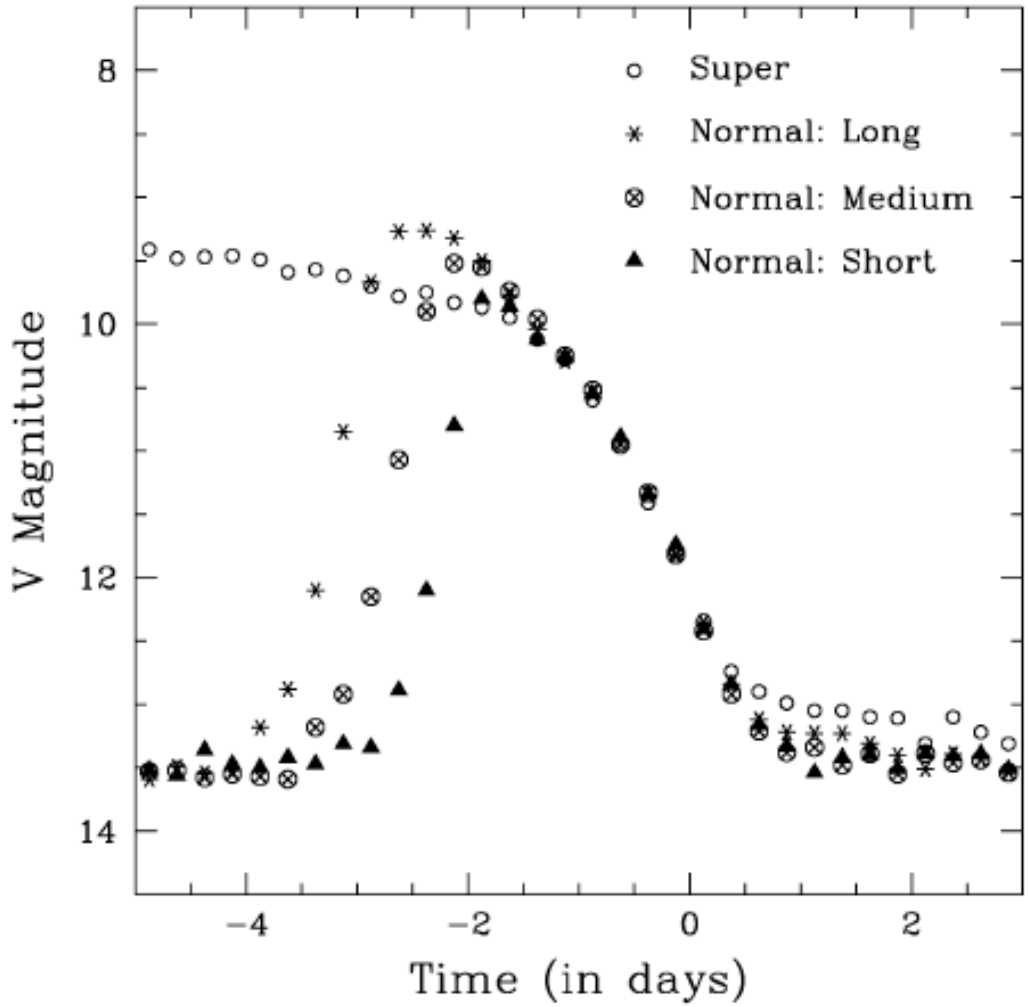

Figure 5. Average profiles of superoutbursts and the three types of normal outburst.

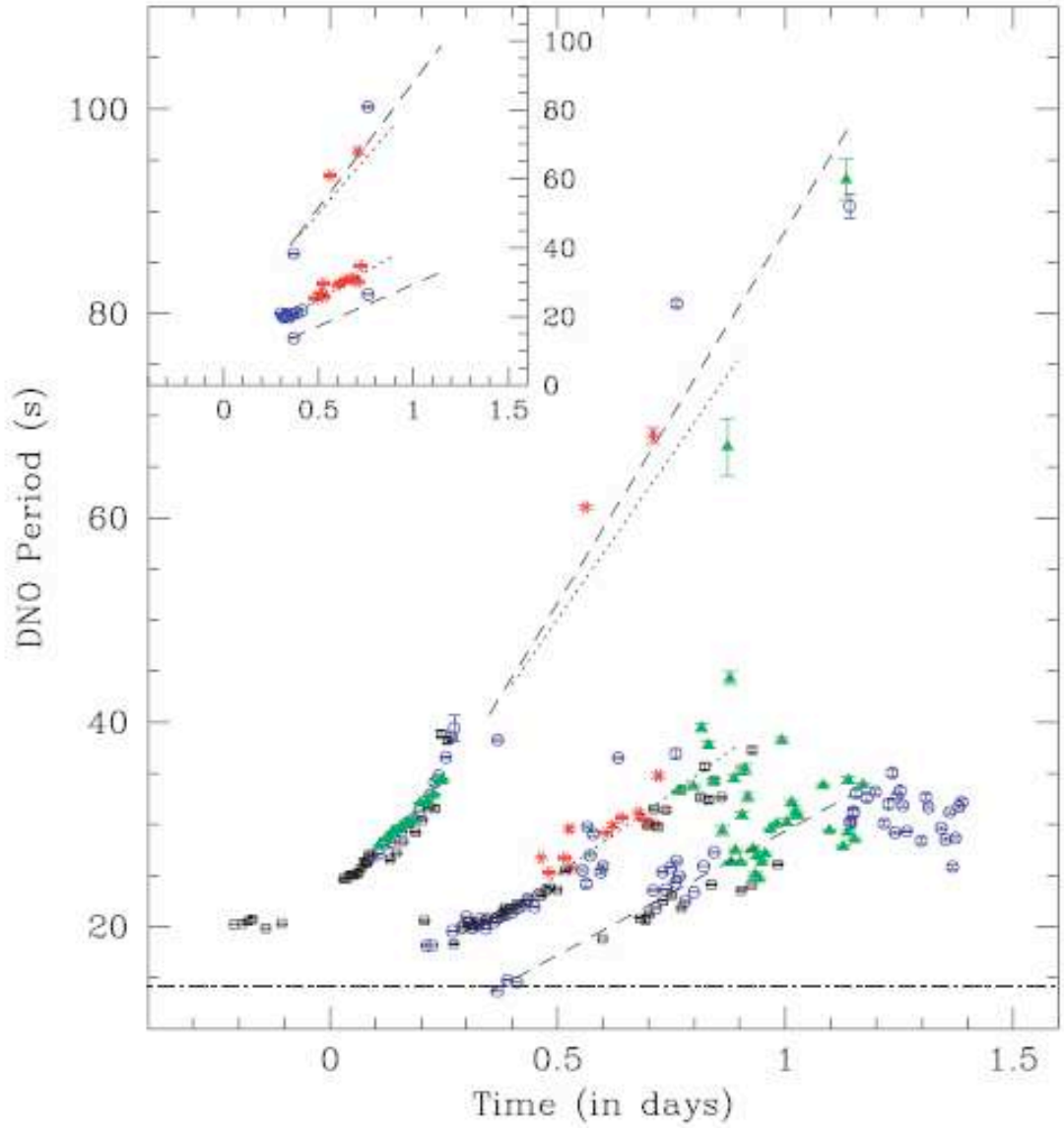
DNO Period (s)
Time (in days)
100
80
60
40
20
0
0.5
1
1.5

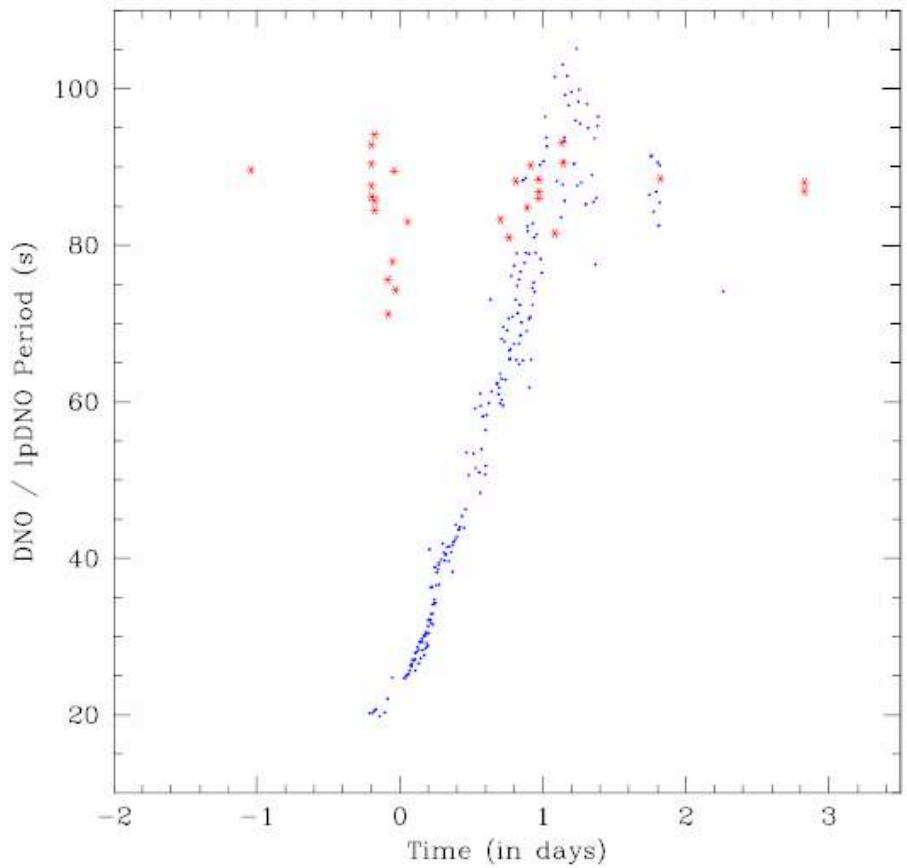

FIGURE 7. Time-evolution of the observed or implied fundamental DNO periods (small dots) and lpDNO periods (asterisks).

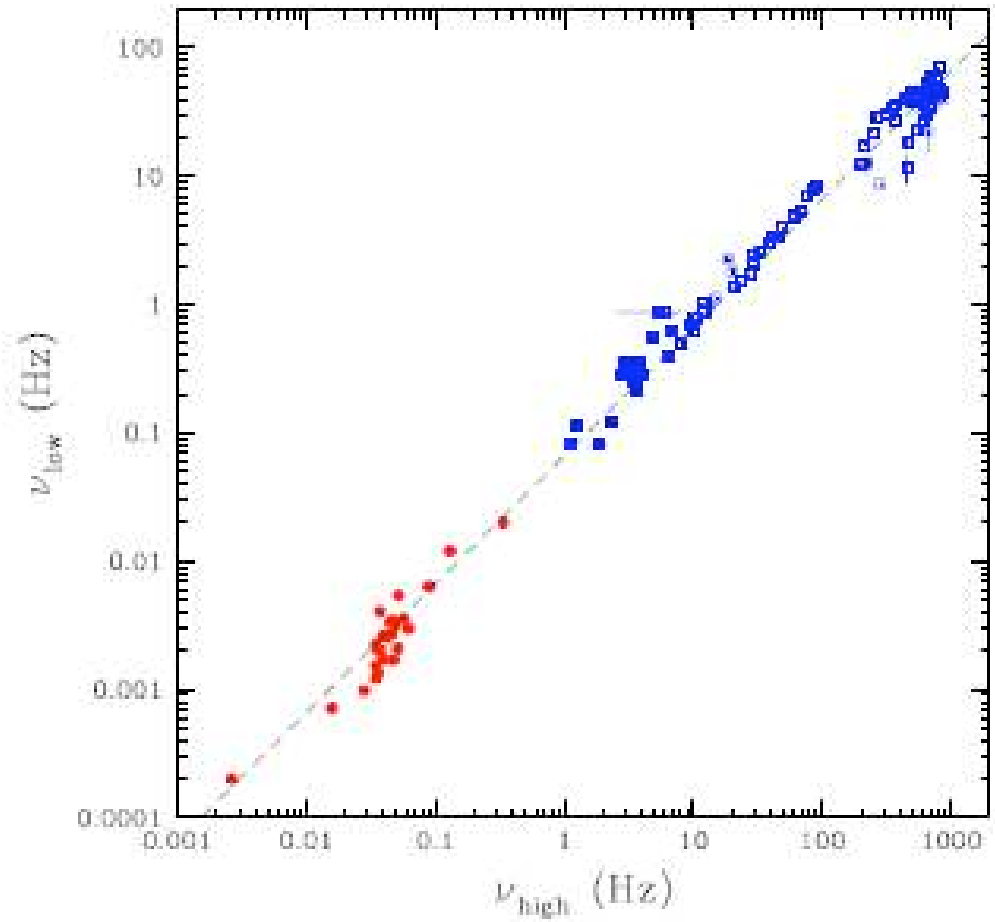

FIGURE 6. An updated version of the two-QPO diagram for X-ray binaries (filled squares: black hole binaries; open squares: neutron star binaries) and 26 CVs (filled circles). Each CV is only shown once in this diagram. The X-ray data are from [17] and were kindly provided by T. Belloni. The dashed line marks $P_{\rm QPO}/P_{\rm DNO} = 15$.

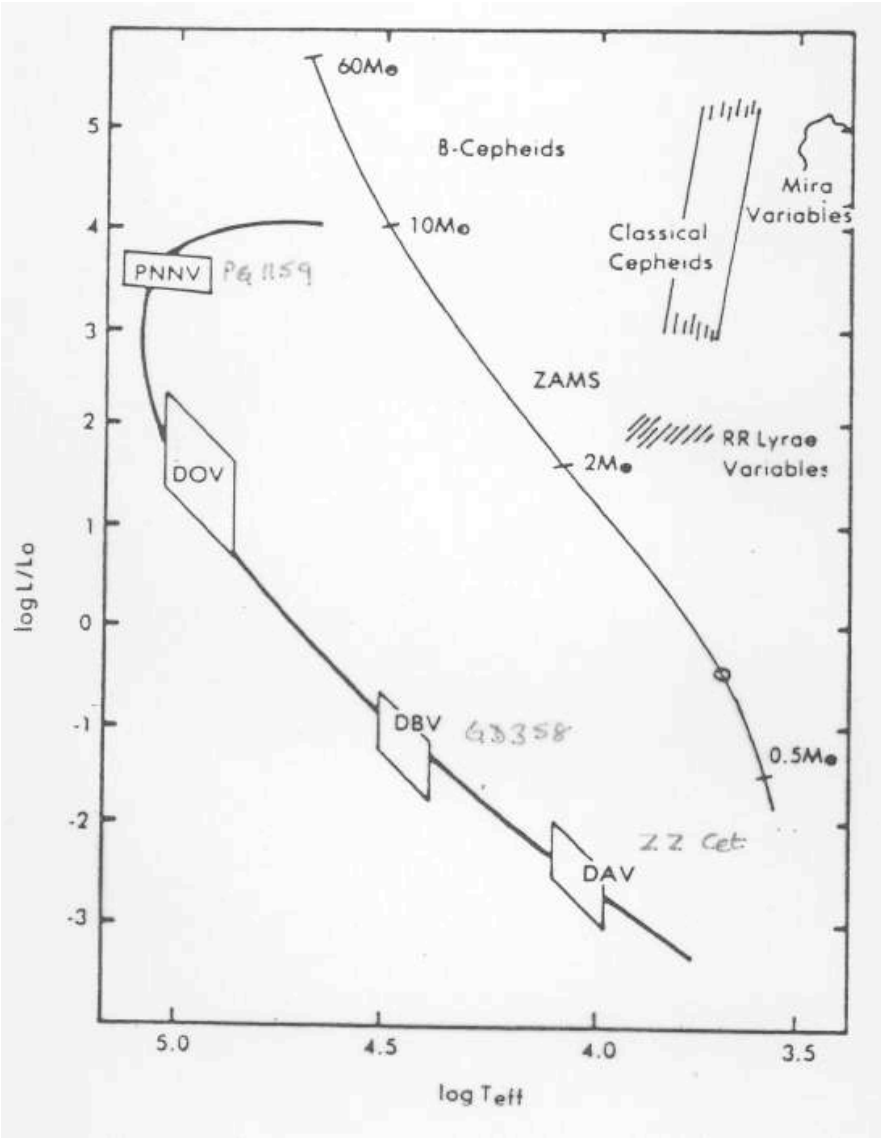
60M⊙
B-Cepheids
Mira
Variables
10M⊙
Classical
Cepheids
PNNV
PG 1159
ZAMS
RR Lyrae
Variables
2M⊙
DOV
DBV
GD358
0.5M⊙
ZZ Cet
DAV
5
4
3
2
1
0
-1
-2
-3
5.0
4.5
4.0
3.5
log L/Lo
log Teff

Figure 8.5. A short section of the light curve of the pulsating white dwarf ZZ Cet (R 548). Each point is a 20-s average of the photon count rate. Beats between the 213-s and 274-s pulsations are clearly seen. From E. L. Robinson, R. E. Nather & J. T. McGraw, *Astrophys. J.*, **210**, 211, 1976.

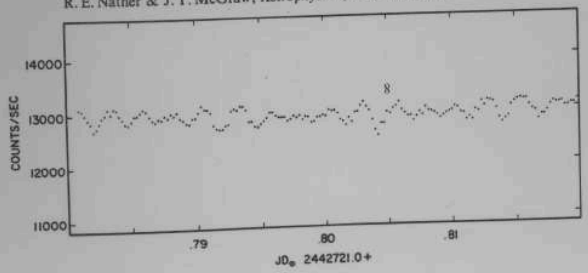

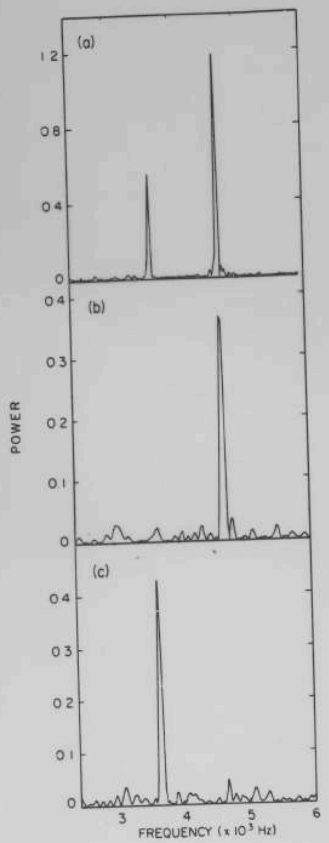

Nonradial Pulsations

For either a "p"- or "g"-type oscillation (which may involve variations in surface radial velocity, brightness, or temperature), a particular mode is characterized by a trio of integers: l, m, and k. The first two correspond to properties that depend, respectively, upon latitude and longitude; varying over the surface, they are "nonradial." In the accompanying illustrations of some simple nonradial modes, the light and dark areas of the stars' surfaces always behave in the opposite manner. For example, the mode $l = 2$ and $m = 0$ corresponds to an oscillation during which the two pole caps are, say, alternately both brighter or both darker than the equatorial belt that separates them. The third number, k specifies the radial overtone of the pulsation.

For nonrotating stars, the period of a p- or g-mode oscillation does not depend upon m. For a given overtone (say $k = 1$, which corresponds to the first overtone for p-modes and to the fundamental for g-modes), the period is longest for the smallest value of l. A p-mode with $l = 0$ is radial, while there are no g-modes with $l = 0$. For l values of one or greater, both p- and g-modes are possible.

The distinction between the two main types of pulsations becomes most dramatic when examining the periods of increasingly high overtones for a given value of the index l. For p-modes, higher overtones have shorter periods. For g-modes, however, the situation is reversed, higher and higher overtones having longer and longer periods. It is this property of g-modes which led Warner and Robinson and Chanmugam to suggest the identification of g-modes with the observed oscillations of ZZ Ceti stars.

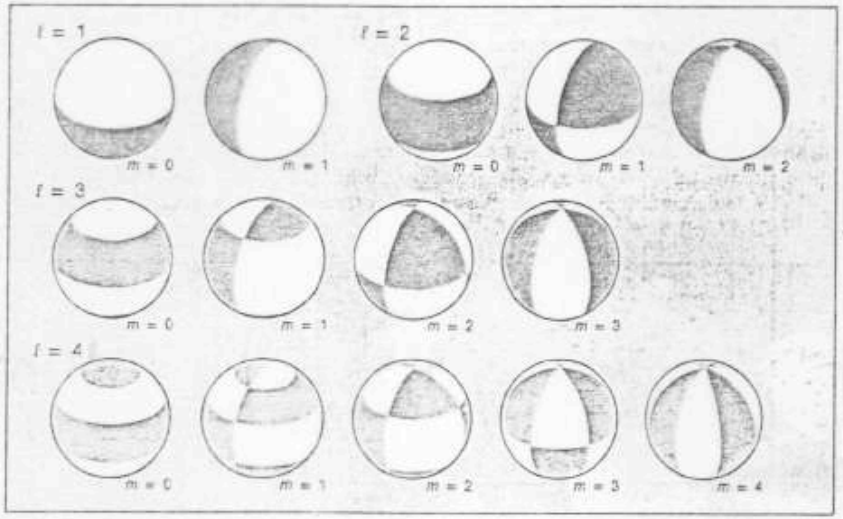

Figure 8.10. Power spectra of two light curves of G 29−38. From J. T. McGraw & E. L. Robinson, *Astrophys. J.*, **200**, L89, 1975.

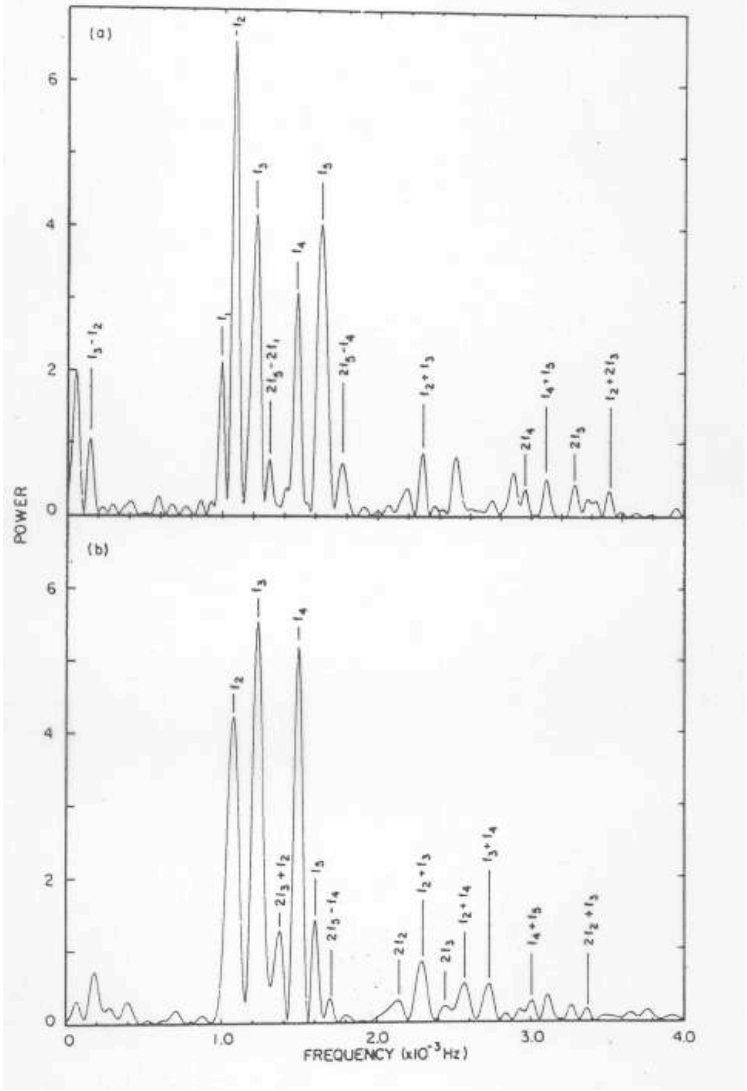

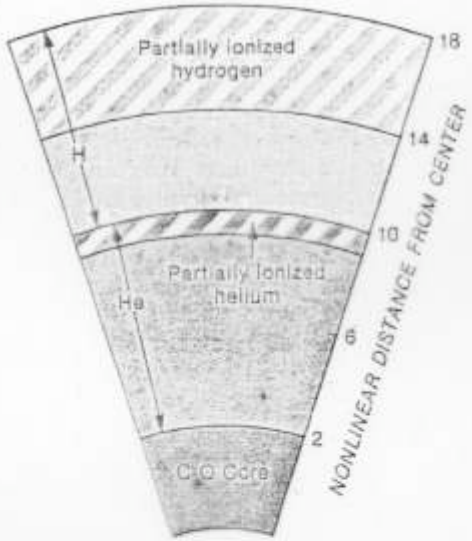

The stratified compositional structure of a ZZ Ceti white dwarf in schematic form. Hydrogen floats to the surface, forming a thin layer a few kilometers deep, comprising one 10-billionth the mass of the star. Below the hydrogen the next heaviest element, helium, forms another thin shell. Its mass is about 100 million times greater than that of hydrogen and represents one percent that of the star. Deeper still is the carbon-oxygen core, comprising most of the variable's mass and volume. The upper parts of the hydrogen and helium regions are both only partially ionized, and changes in the degree of ionization in these zones provide the driving mechanisms which excite the star's pulsations.

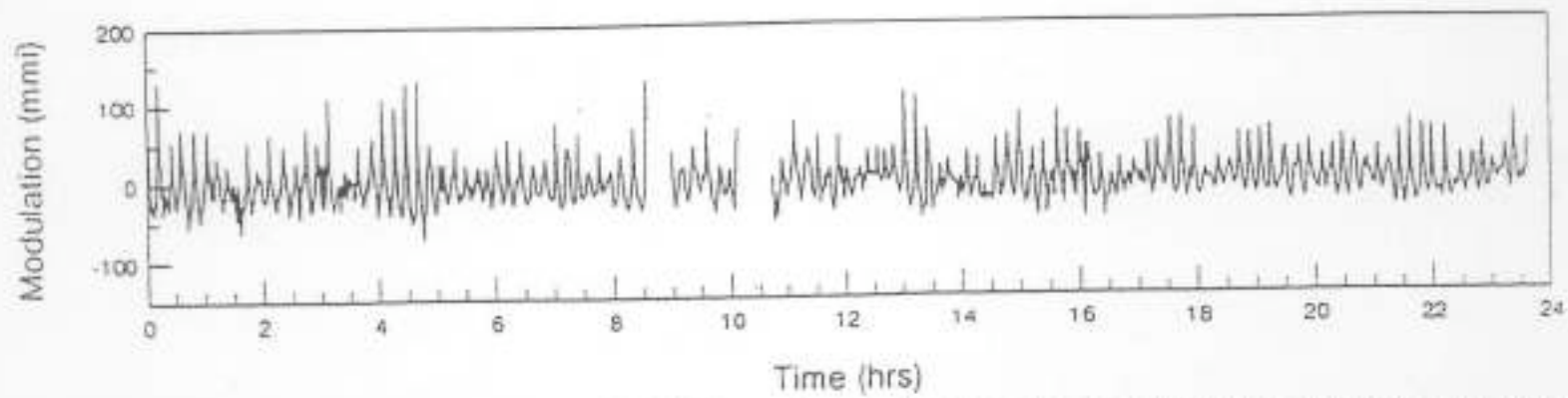

FIG. 1.—Light curve of GD 358 from the central 24 hours of the WET run, after sky effects have been removed and runs from individual telescopes have been combined, in units of millimodulation intensity (mmi).

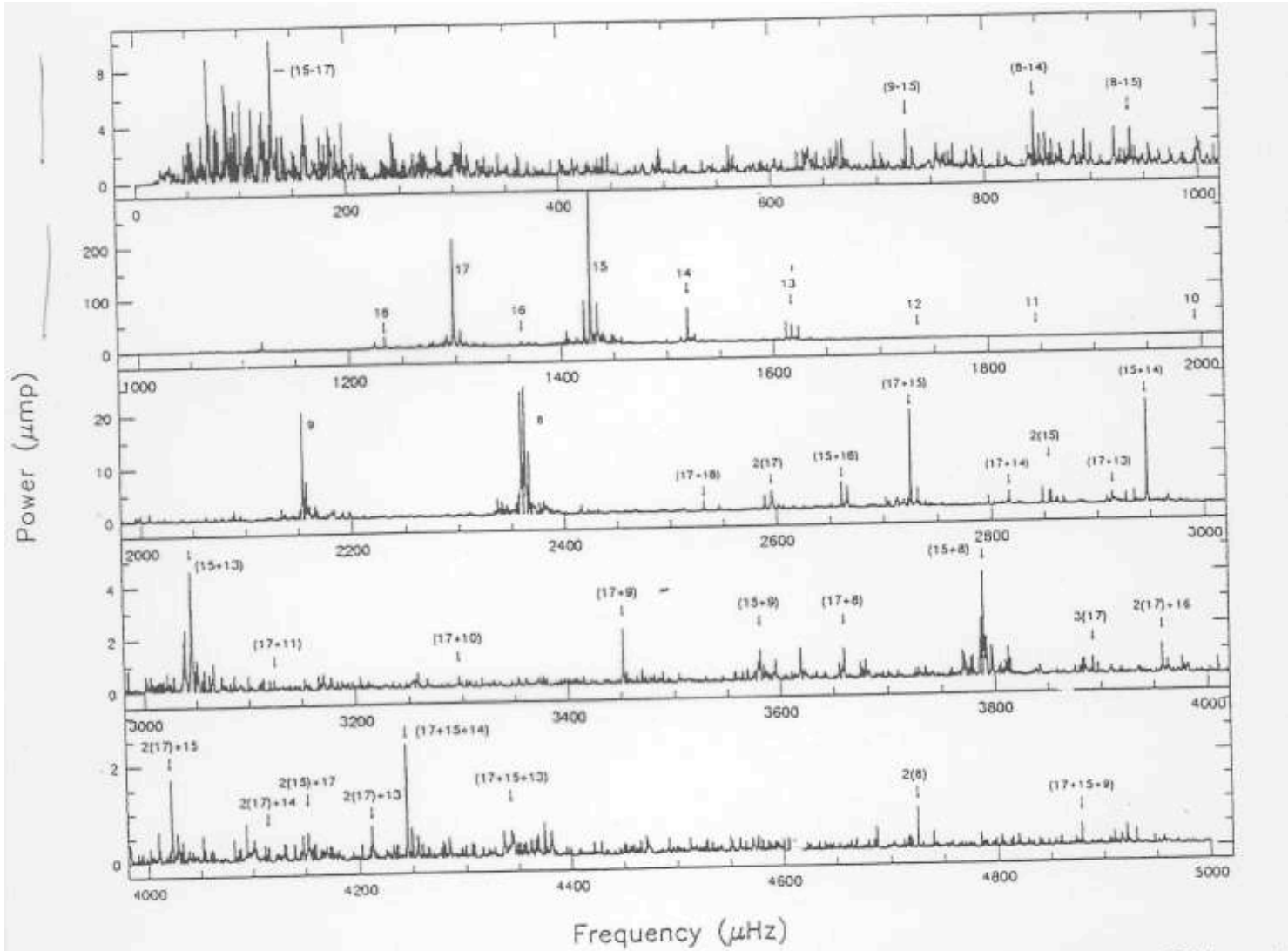

l power spectrum of GD 358. The different scales for each panel attempt to accommodate the large dynamic range present. Triplets are l
ling k-value, and the sum and difference frequencies are labeled with the k-values for the triplets which combine to form them.

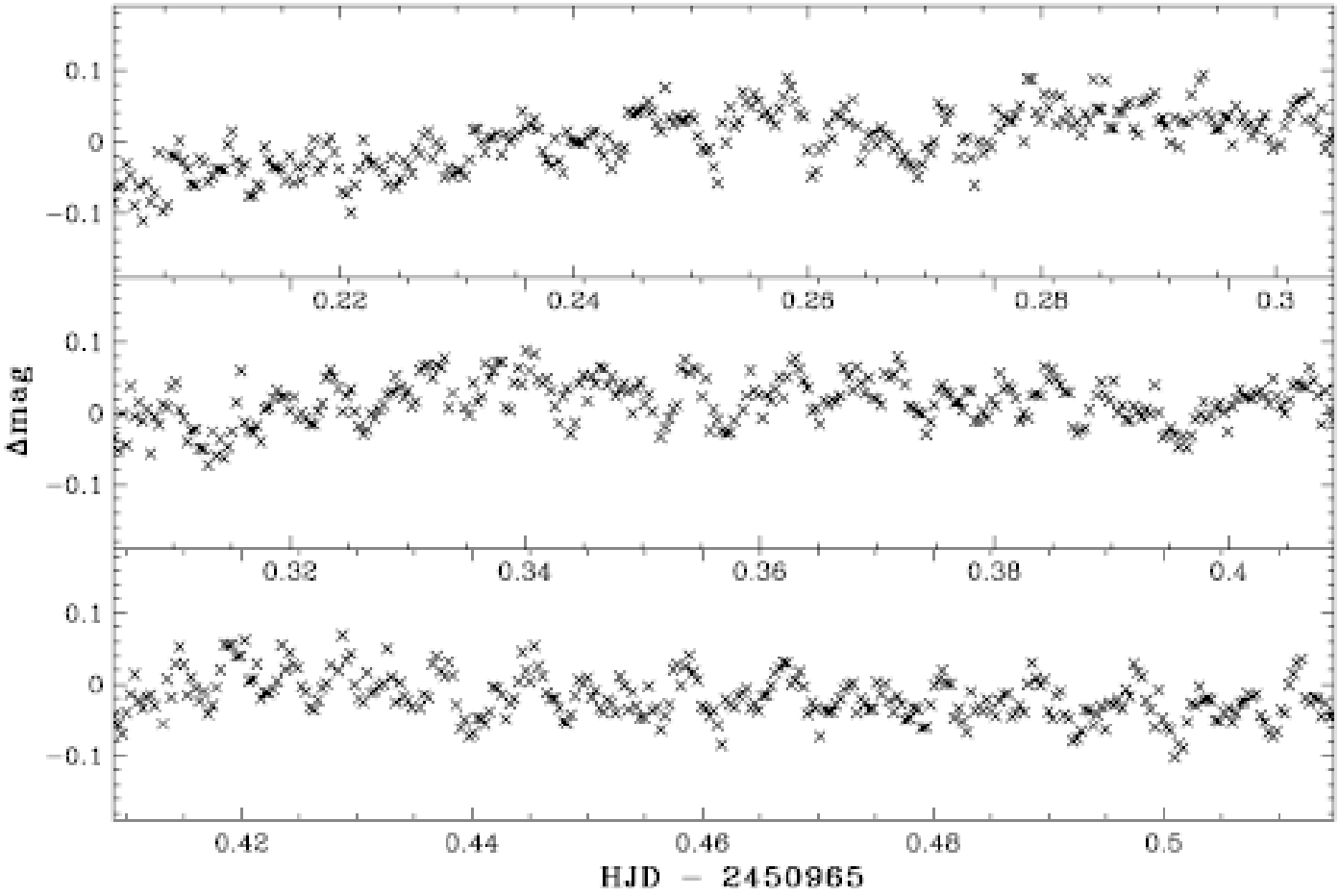

Figure 1. A sample of the light curve of GW Lib, obtained with the SAAO 0.75-m telescope on 1998/31/05.

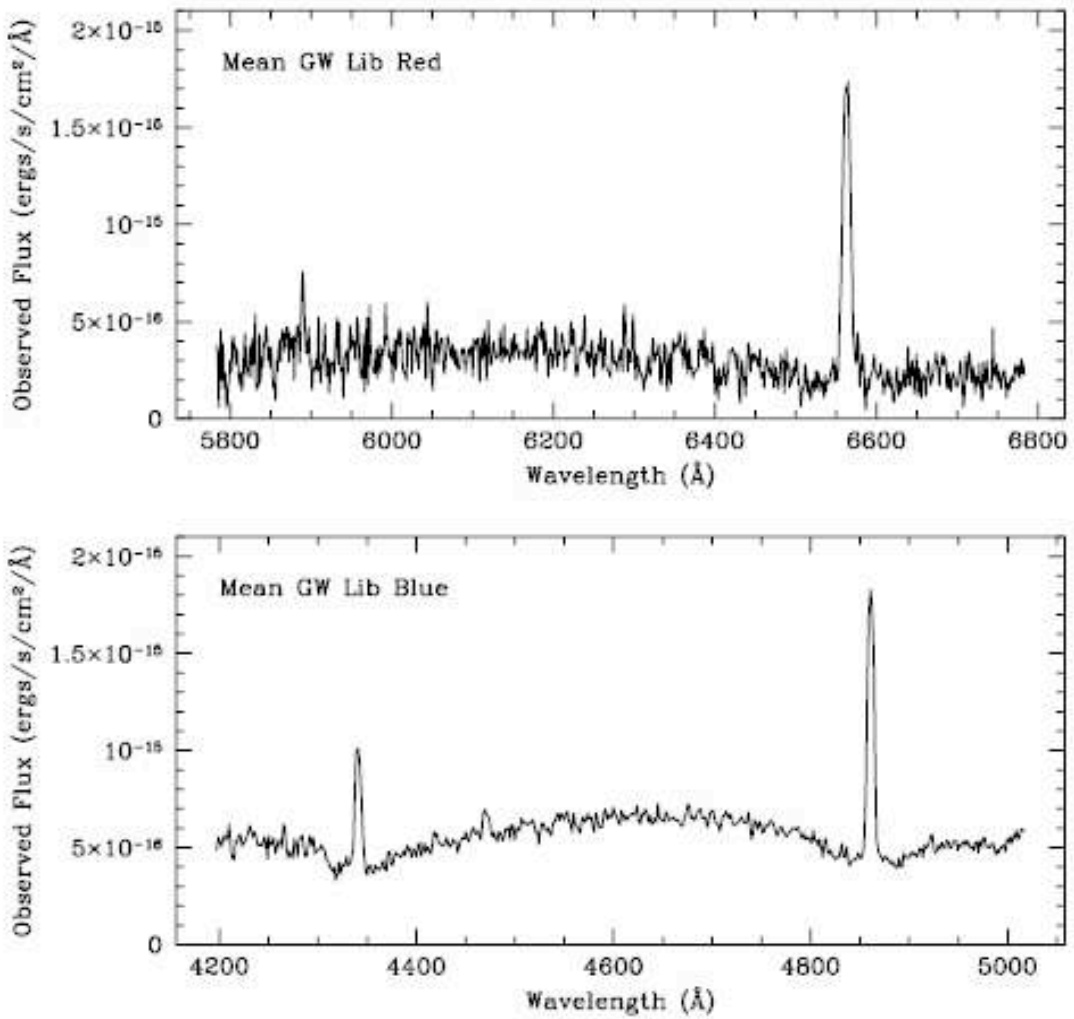

FIG. 1.—Mean spectrum in blue and red for the night of April 1

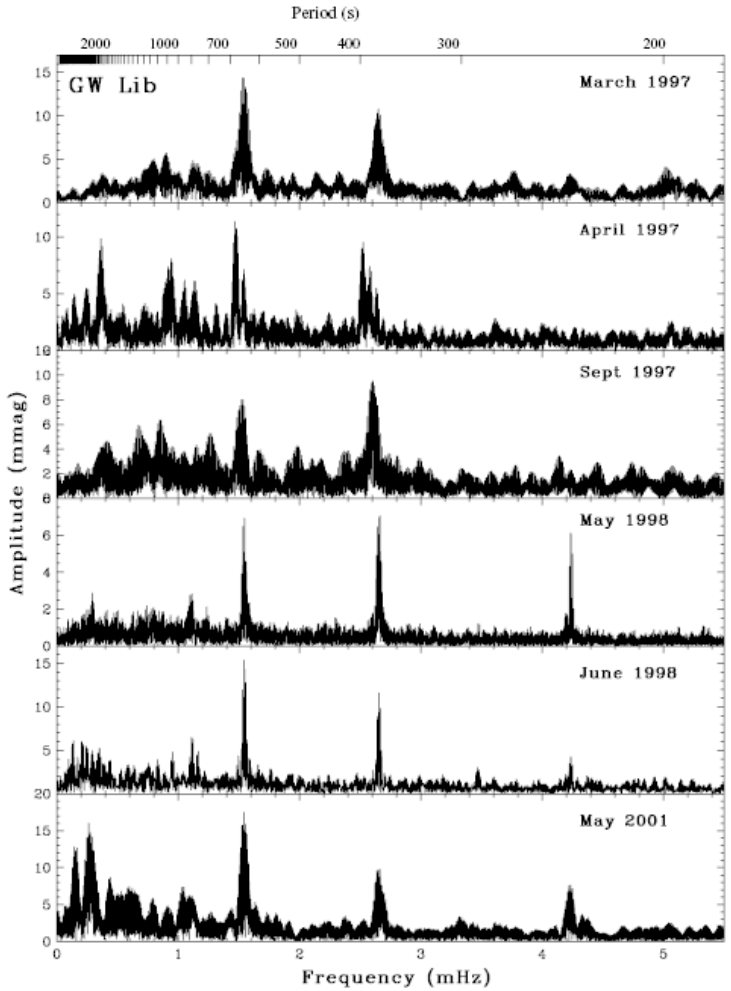

Figure 2. The amplitude spectra of GW Lib from six observing campaigns from 1997 March to 2001 May. The light curves were prepared by fitting and removing linear and low-frequency trends.

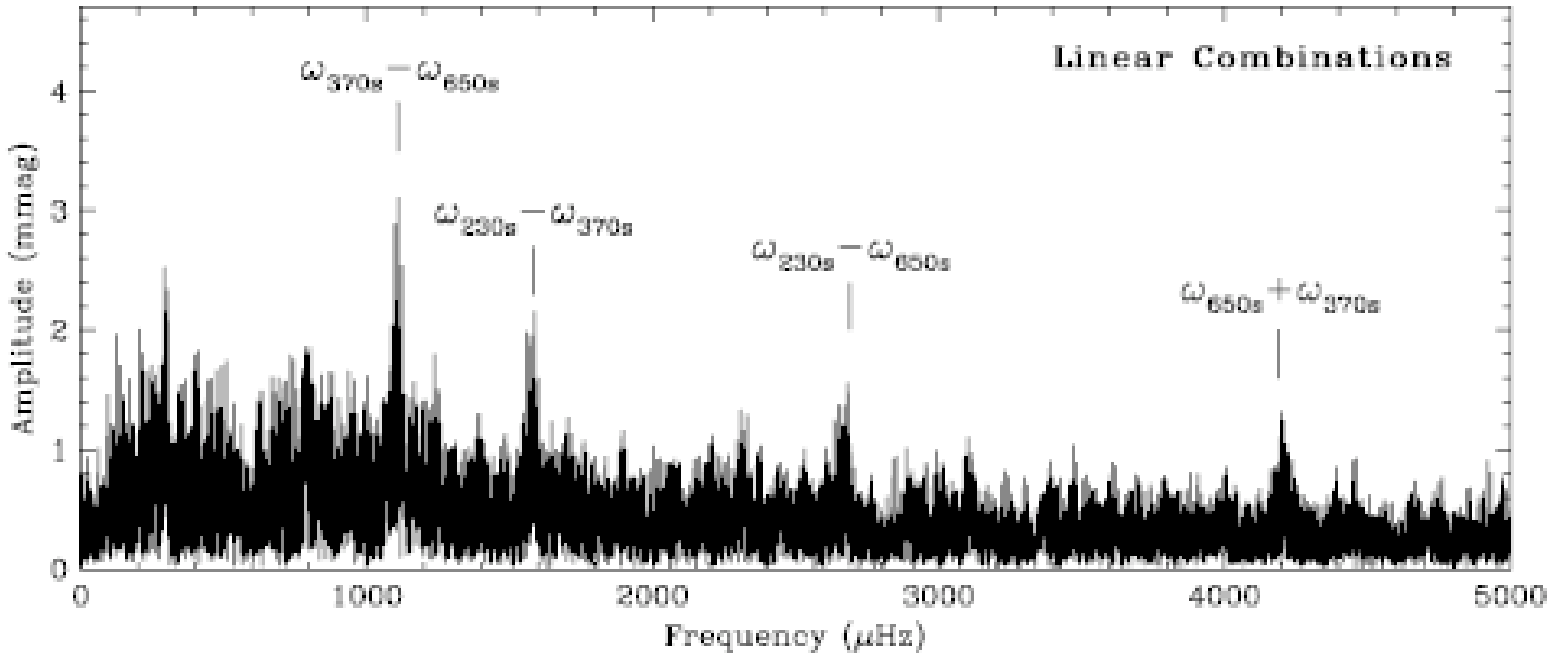

Figure 7. Linear combination modes in the residuals of the 98May&June light curves after prewhitening with all the components of the 650-, 370- and 230-s modes.

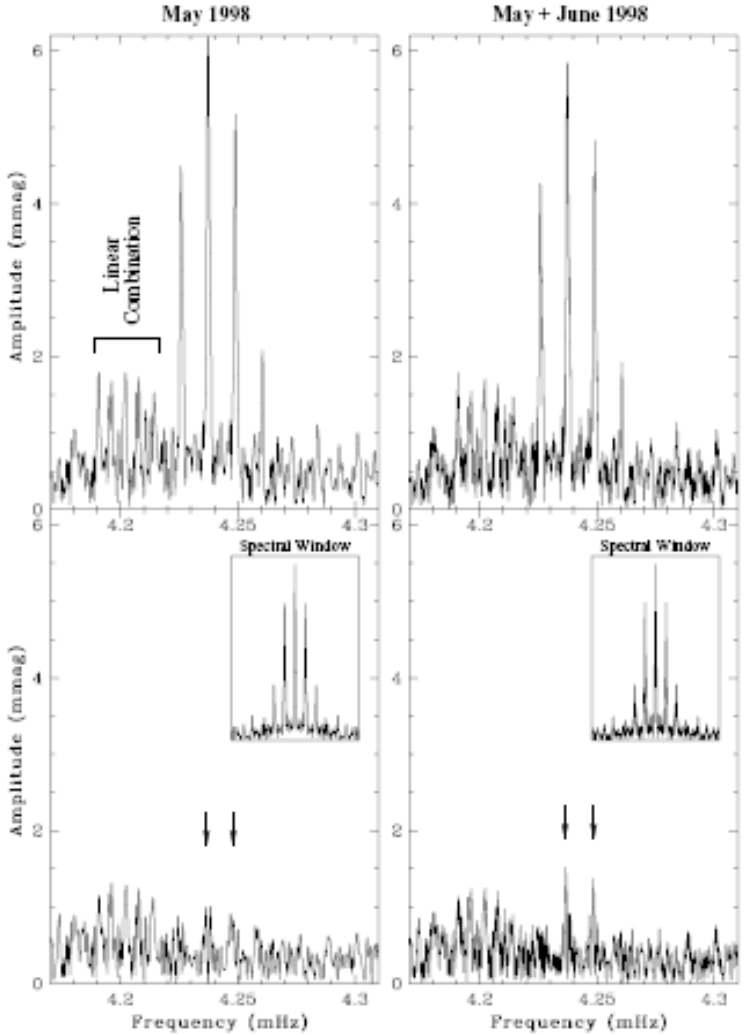

Figure 4. The 230-s mode. In the amplitude spectrum of the 98May data alone, this feature appears to be a single mode (left). However, with the addition of three nights in 1998 June, the baseline is sufficiently extended to reveal a second, low-amplitude mode after prewhitening with the dominant mode (right). (The 'bump' left of centre is a linear combination mode.)

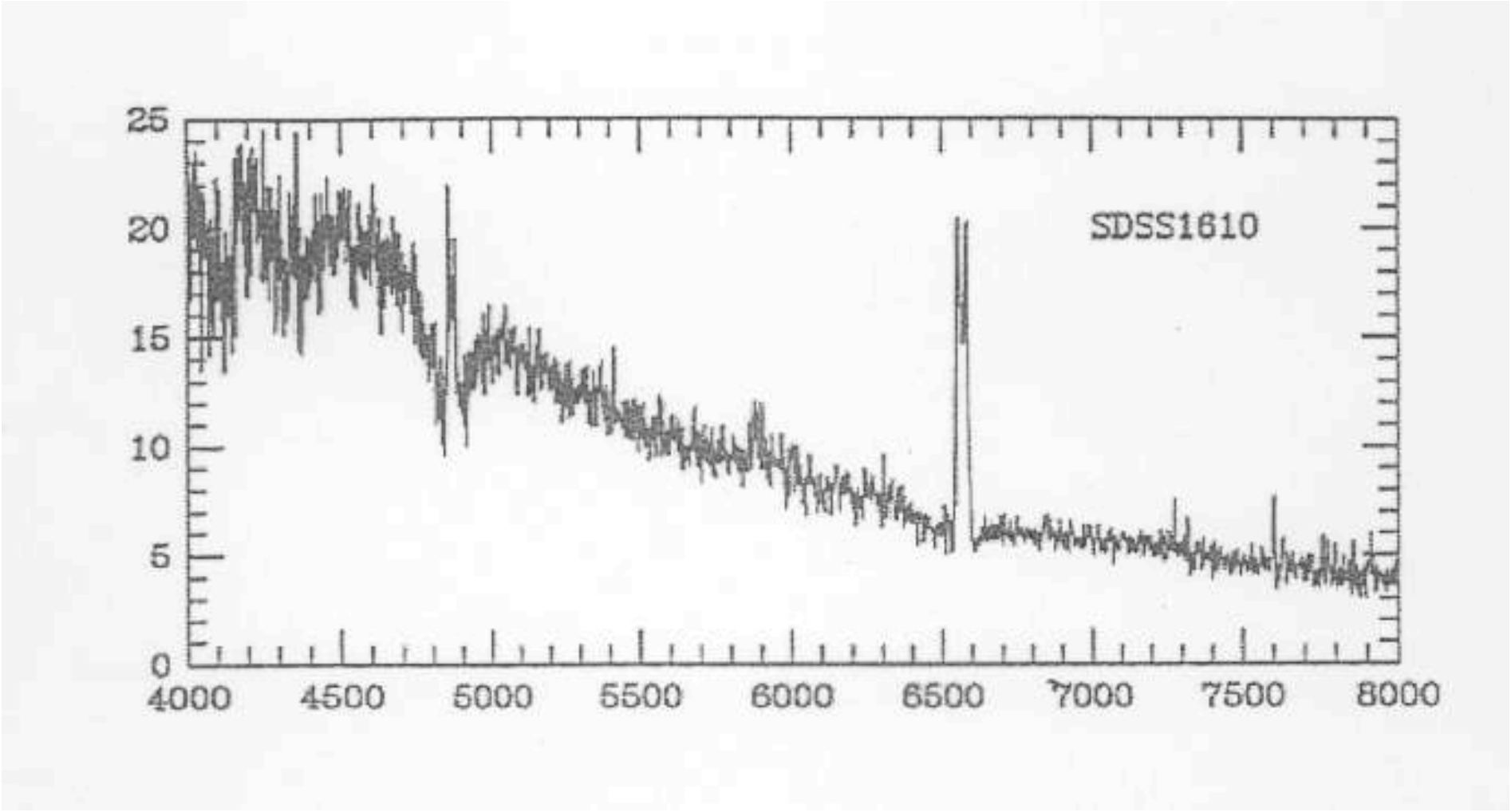
SDSS1610
25
20
15
10
5
0
4000
4500
5000
5500
6000
6500
7000
7500
8000

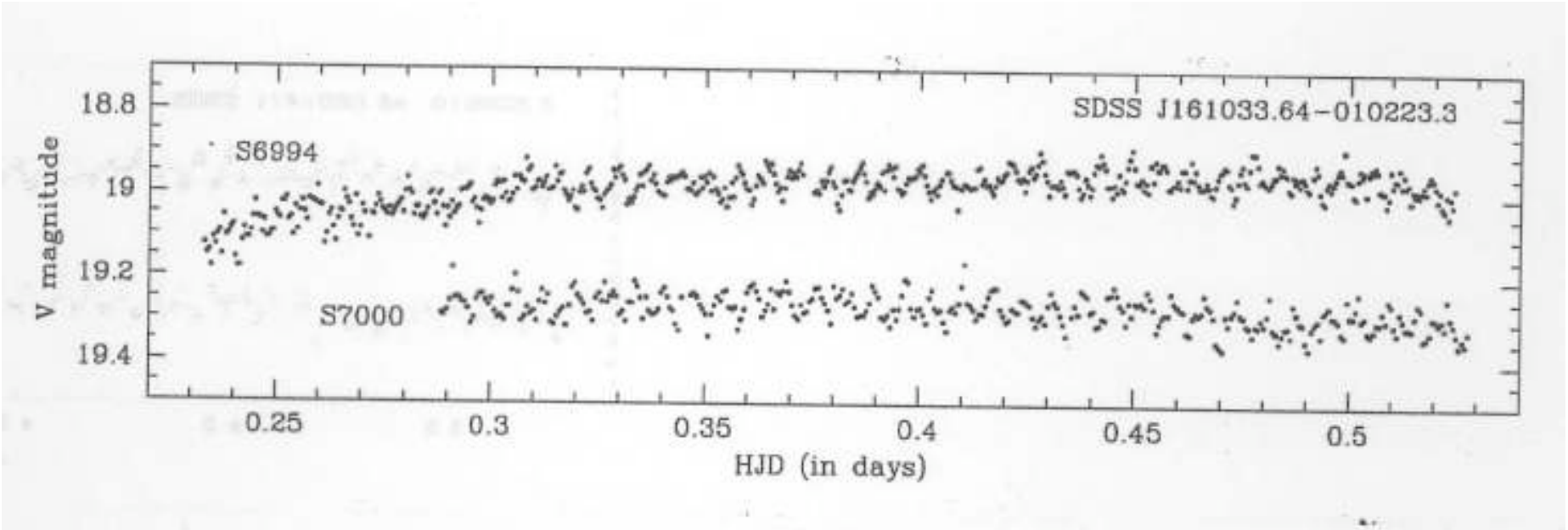
SDSS J161033.64−010223.3
S6994
S7000
V magnitude
18.8
19
19.2
19.4
0.25
0.3
0.35
0.4
0.45
0.5
HJD (in days)

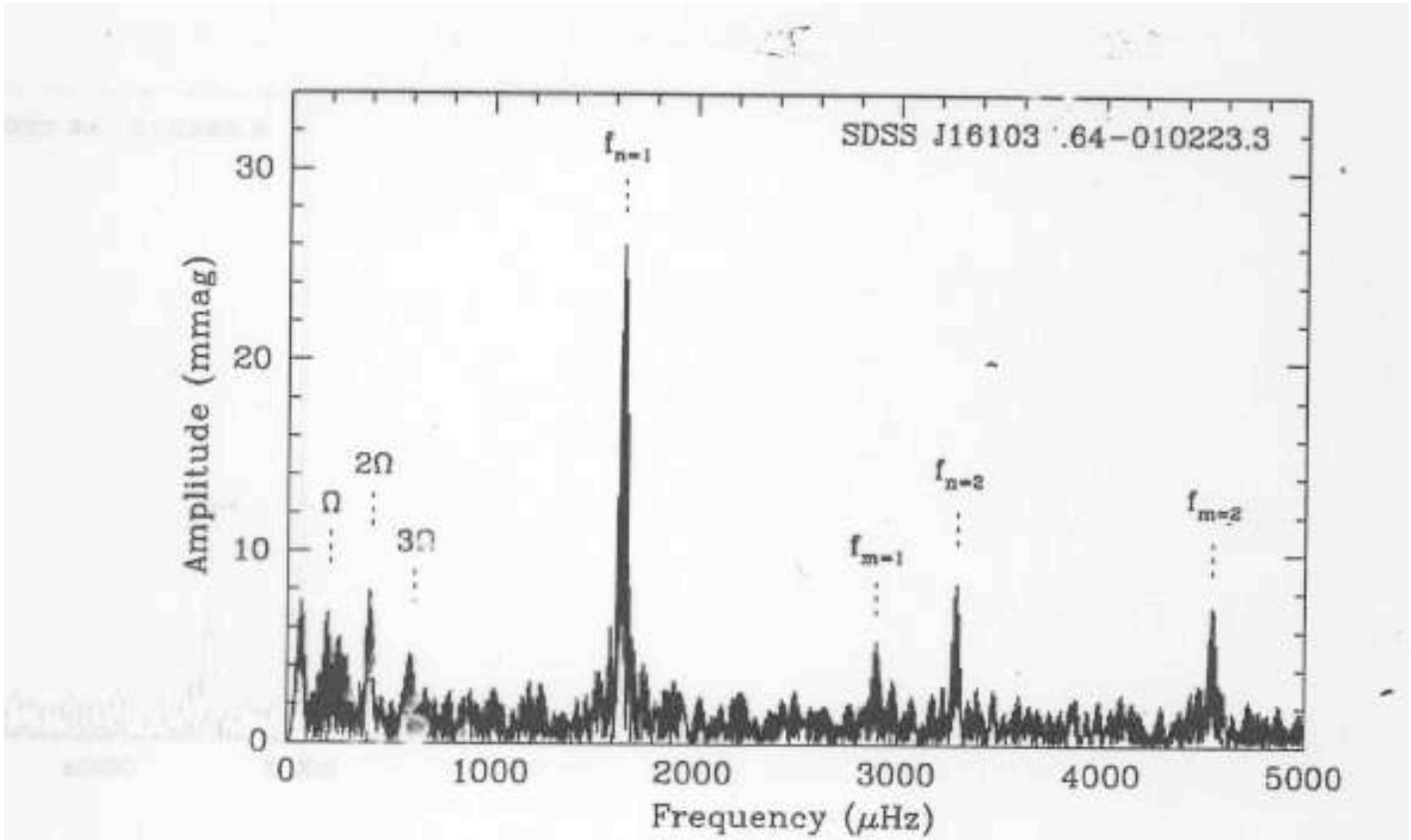

P ~ 221s, 304s, 345s, 607s

The Known ZZ Cet WDs in CVs:

Object	P_{orb}(min)	Mag	Periods	Outbursts	T_{WD}
GW Lib	77	17	230, 370, 650	1983	14700
PQ And	79-81	19	634, 1263	1938, 1967, 1988	12000[opt]
SDSS1610	81	19	221, 304, 345, 607	--	14500
HS2331	81	17	310, 336, 419	--	10500
SDSS1339	83	18	642	--	12500[opt]
SDSS0131	98	18	260, 335, 595	--	14500
REJ1255	119	19	668, 1236, 1344	1994	13000[opt]
SDSS2205	--	20	330, 475, 575	--	15000
SDSS0745	--	19	647, 1010	--	
SDSS2143	--	16	616	--	